Article

Enantioselective Synthesis of Six-Membered Palladacycles Having Metal-Bound Stereogenic Carbons: Isolation and Reactivity of Palladacycles Containing Readily Accessible β-Hydrogens

Brenda J. Burke, and Larry E. Overman

J. Am. Chem. Soc., **2004**, 126 (51), 16820-16833• DOI: 10.1021/ja045047p • Publication Date (Web): 07 December 2004

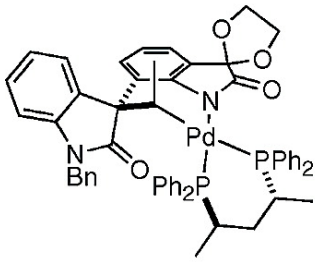

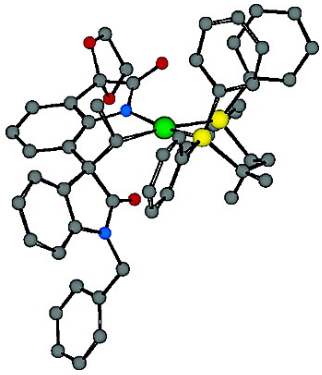

More About This Article

Additional resources and features associated with this article are available within the HTML version:

- Supporting Information
- Access to high resolution figures
- Links to articles and content related to this article
- Copyright permission to reproduce figures and/or text from this article

View the Full Text HTML

J|A|C|S
ARTICLES
Published on Web 12/07/2004

Enantioselective Synthesis of Six-Membered Palladacycles Having Metal-Bound Stereogenic Carbons: Isolation and Reactivity of Palladacycles Containing Readily Accessible β-Hydrogens

Brenda J. Burke and Larry E. Overman*

Contribution from the Department of Chemistry, 516 Rowland Hall, University of California, Irvine, California 92697-2025

Received August 17, 2004; E-mail: leoverma@uci.edu

Abstract: Five enantiopure palladacycles containing palladium bonded to a stereogenic carbon and an N-coordinated oxindole were synthesized by the reaction of alkenyl aryl triflates **2** and **9** with Pd(0) bisphosphine complexes. Two palladacyclic complexes, **3β** and **10α**, were characterized by single-crystal X-ray crystallography. The reactivity of neutral palladacycles **3β** and **10β** was studied in detail. These unusual palladium alkyls, which have three accessible β-hydrogens, are thermally stable at temperatures as high as 120 °C. At higher temperature, or at room temperature in the presence of weak acids, these complexes epimerize at the stereogenic carbon bonded to palladium. The mechanism of the acid-promoted epimerization was studied in detail. During this epimerization, cationic palladium alkyls **13**/**14** and **33** and cationic palladium hydride alkene complexes **31** and **32** are in rapid equilibrium.

Introduction

Palladacycles are a well-studied class of organopalladium complexes in which the palladium atom is contained within a ring. The first palladacycle was reported in 1965 when A. C. Cope published the carbopalladation of azobenzene with $PdCl_2$ to generate **1** (eq 1).[1] Since his discovery, hundreds of palladacycles have been reported; the most common have five-membered rings, although ring sizes from 3 to 10 are known.

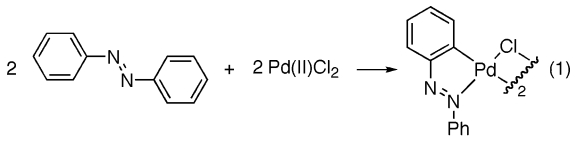

1

Early in their history, palladacycles were classified as catalytically inactive complexes,[2] but over the past decade they have proven themselves to be convenient and efficient catalyst precursors for the construction of both C−C and C−heteroatom bonds. Palladacyclic catalysts have been successfully employed in Heck[3] and Suzuki couplings,[4] Buchwald−Hartwig aminations,[5] and Stille reactions.[6] In addition to being important precatalysts, palladacycles are intermediates in many of these and other palladium-mediated reactions.

In the course of our studies to develop an enantioselective total synthesis of the polypyrrolidinoindoline alkaloid quadrigemine C,[7] we isolated a novel six-membered palladacycle, **3**[8] ([P−P] = (*R*)-(+)-2,2′-bis(diphenylphosphino)-1,1′-binaphthyl, (*R*)-BINAP)[9] (Scheme 1). This product was formed in moderate yield when the asymmetric Heck cyclization of **2** was

Scheme 1

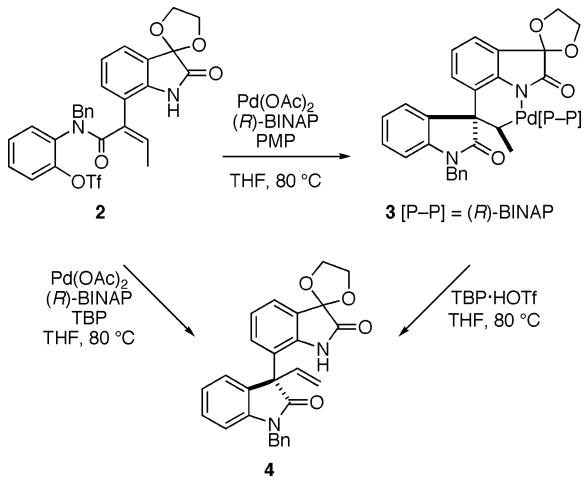

2 **3** [P–P] = (*R*)-BINAP

4

(1) Cope, A. C.; Siekman, R. W. *J. Am. Chem. Soc.* **1965**, *87*, 3272−3273.
(2) For a review of the role of palladacycles in C−C and C−heteroatom bond-forming reactions, see: Bedford, R. B. *Chem. Commun.* **2003**, 1787−1796.
(3) Herrmann, W. A.; Brossmer, C.; Öfele, K.; Reisinger, C.-P.; Priermeier, T.; Beller, M.; Fischer, H. *Angew. Chem.* **1995**, *34*, 1844−1848.
(4) Beller, M.; Fischer, H.; Herrmann, W. A.; Öfele, K.; Brossmer, C.; *Angew. Chem.* **1995**, *34*, 1848−1852.
(5) (a) Wolfe, J. P.; Åhman, J.; Sadighi, J. P.; Singer, R. A.; Buchwald, S. L. *Tetrahedron Lett.* **1997**, *38*, 6367−6370. (b) Mann, G.; Hartwig, J. F.; Driver, M. S.; Fernández-Rivas, C. *J. Am. Chem. Soc.* **1998**, *120*, 827−828.
(6) Muñoz, M. P.; Martín-Matute, B.; Fernández-Rivas, C.; Cárdenas, D. J.; Echavarren, A. M. *Adv. Synth. Catal.* **2001**, *343*, 338−342.
(7) An enantioselective total synthesis of quadrigemine C has since been completed by an alternate route: Lebsack, A. D.; Link, J. T.; Overman, L. E.; Stearns, B. A. *J. Am. Chem. Soc.* **2002**, *124*, 9008−9009.
(8) Oestreich, M.; Dennison, P. R.; Kodanko, J. J.; Overman, L. E. *Angew. Chem.* **2001**, *40*, 1439−1442.
(9) Miyashita, A.; Yasuda, A.; Takaya, H.; Toriumi, K.; Ito, T.; Souchi, T.; Noyori, R. *J. Am. Chem. Soc.* **1980**, *102*, 7932−7934.

10.1021/ja045047p CCC: $27.50

conducted with 1 equiv of $Pd(OAc)_2$ and 1.5 equiv of (*R*)-BINAP in the presence of the relatively strong base 1,2,2,6,6-pentamethylpiperidine (PMP, pK_a of the conjugate acid in acetonitrile = 18.7).[10] When a similar reaction was carried out in the presence of the weaker base 2,6-di-*tert*-butylpyridine (TBP, pK_a of the conjugate acid in acetonitrile = 11.8),[11] Heck product **4**, rather than palladacycle **3**, was isolated. Palladacycle **3** was shown to be stable in the presence of PMP hydrotriflate (PMP·HOTf), but rapidly converted to **4** in the presence of 2,6-di-*tert*-butylpyridine hydrotriflate (TBP·HOTf).

Six-membered palladacycles such as **3** that are stable at room temperature and contain a σ-bond between palladium and an sp^3 carbon having β-hydrogens are rare, particularly so when the sp^3 carbon is stereogenic.[12] Prior to our disclosure of **3**, there were no examples of six-membered palladacycles having β-hydrogens attached to a freely rotating sp^3 carbon external to the palladacyclic ring, although several are known in the four- and five-membered palladacycle series. The asymmetric synthesis of palladacycle **3** depicted in Scheme 1 represents a marked improvement over previous syntheses of enantiomerically enriched palladacycles containing palladium bonded to a stereogenic carbon, all of which required a low-yielding resolution step.[13]

In this account, the synthesis and full characterization of a series of enantiomerically enriched palladacycles, **3** and congeners, are described, along with studies that define the reactivity of these unique complexes.

Results

Palladacycle Synthesis. The (*Z*)-2-pentenoyl precursor **9** was constructed from *N*-benzyloxazolinone **5**[14] following a general route previously developed in our laboratories (Scheme 2).[8,15] Addition of oxazolinone **5** to 1-lithiobutyne at −78 °C, followed by trapping the resultant phenoxide with *N*-phenyltriflimide, proceeded efficiently to provide alkynyl amide **6**. Regioselective hydrostannylation of this product with tributyltinhydride in the presence of catalytic $Pd(PPh_3)_4$ afforded *E* vinyl stannane **7** in 91% yield.[16] Stille coupling of stannane **7** with the ketal-protected 7-iodoisatin **8**[17] delivered aryl triflate **9** in good yield.[18]

Reactions of unsaturated aryl triflates **2** and **9** with 1 equiv of $Pd(OAc)_2$, 2 equiv of BINAP or 2,4-(bisdiphenylphosphinopentane) (BDPP),[19] and 4 equiv of PMP proceeded with high diastereoselection (≥93:7 β:α CH_2R) to give chiral palladacycles **3**, ***ent*-3**, **10**, ***ent*-10**, and **11** in high yields (Table 1).[20] As reported earlier,[8] reaction of aryl triflate **2** with $Pd(OAc)_2$, (*R*)-BINAP, and the acid scavenger PMP yielded palladacycle **3**. When this reaction was carried out in *N*,*N*-dimethylacetamide (DMA) with 2.0 equiv of (*R*)-BINAP at 80 °C, palladacycle **3** was isolated in 95% yield as a 96:4 mixture of β:α-methyl epimers (entry 1). These epimers, **3*β*** and **3α**, could be separated by careful silica gel chromatography. The nomenclature β and α will be used to designate the epimer at the carbon adjacent to palladium, with the β-substituent being on the face of the palladacyclic ring opposite the carbonyl group of the *N*-benzyloxindole substituent. Employing (*S*)-BINAP, we found that the corresponding enantiomeric palladacycle ***ent*-3** was isolated in 84% yield as a 93:7 mixture of epimers (entry 2).

Palladacyclization of **2** with the more electron-rich bisphosphine (*R*,*R*)-BDPP proceeded optimally at 70 °C in DMA, to provide palladacycle **10** in 94% yield as a 96:4 mixture of β:α-methyl epimers (entry 3). Epimer **10*β*** could be isolated in pure form by careful silica gel chromatography, but the minor epimer **10α** was not isolated as it was not detected after flash chromatography. Similar results were observed with the enantiomeric BDPP ligand (entry 4).

Palladacycle precursor **9**, containing a (*Z*)-2-pentenoyl fragment, reacted with $Pd(OAc)_2$ and (*R*)-BINAP to give palladacycle **11** in 67% isolated yield as an inseparable 94:6 mixture of β:α-ethyl epimers (entry 5). The lower yield observed in this case resulted from a competing β-hydride elimination pathway to generate Heck product **12**, which was isolated in 17% yield and 93% ee.[21] Numerous other bidentate and monodentate chiral

Scheme 2

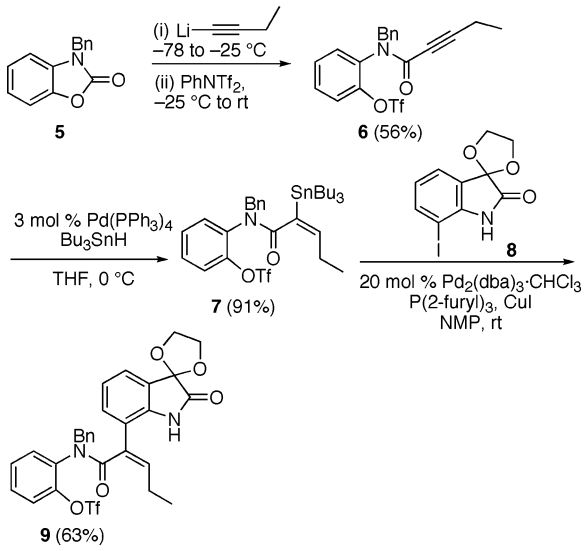

(10) Dworniczak, M.; Leffek, K. T. *Can. J. Chem.* **1990**, *68*, 1657−1661.
(11) Schlesener, C. J.; Amatore, C.; Kochi, J. K. *J. Am. Chem. Soc.* **1984**, *106*, 7472−7482.
(12) (a) A search of the CA Registry file finds 13 examples; only one of these is in the Cambridge Structural Data Base. (b) For a palladacycle isolated from an intramolecular Heck reaction that has a primary C−Pd σ-bond, see: Clique, B.; Fabritius, C.-H.; Couturier, C.; Monteiro, N.; Balme, G. *Chem. Commun.* **2003**, *2*, 272−273.
(13) (a) Sokolov, V. I.; Sorokina, T. A.; Troitskaya, L. L.; Solovieva, L. I.; Reutov, O. A. *J. Organomet. Chem.* **1972**, *36*, 389−390. (b) Maassarani, F.; Pfeffer, M.; Le Borgne, G.; Jastrzebski, J. T. B. H.; van Koten, G. *Organometallics* **1987**, *6*, 1111−1118. (c) Dunina, V. V.; Golovan, E. B.; Kazakova, E. I.; Potapov, G. P.; Beletskaya, I. P. *Metalloorg. Khim.* **1991**, *4*, 1391−1396. (d) Pereira, M. T.; Pfeffer, M.; Rotteveel, M. A. *J. Organomet. Chem.* **1989**, *375*, 139−145. (e) Spencer, J.; Maassarani, F.; Pfeffer, M.; DeCian, A.; Fischer, J. *Tetrahedron: Asymmetry* **1994**, *5*, 321−324.
(14) Ucar, H.; Van derpoorten, K.; Cacciaguerra, S.; Spampinato, S.; Stables, J. P.; Depovere, P.; Isa, M.; Masereel, B.; Delarge, J.; Poupaert, J. H. *J. Med. Chem.* **1998**, *41*, 1138−1145.
(15) Dounay, A. B.; Hatanaka, K.; Kodanko, J. J.; Oestreich, M.; Overman, L. E.; Pfeifer, L. A.; Weiss, M. M. *J. Am. Chem. Soc.* **2003**, *125*, 6261−6271.
(16) (a) Zhang, H. X.; Guibé, F.; Balavoine, G. *J. Org. Chem.* **1990**, *55*, 1857−1867. (b) Cochran, J. C.; Bronk, B. S.; Terrence, K. M.; Phillips, H. K. *Tetrahedron Lett.* **1990**, *31*, 6621−6624. (c) Betzer, J.-F.; Delaloge, F.; Muller, B.; Pancrazi, A.; Prunet, J. *J. Org. Chem.* **1997**, *62*, 7768−7780.
(17) (a) Farina, V.; Krishnan, B. *J. Am. Chem. Soc.* **1991**, *113*, 9585−9595. (b) Farina, V.; Kapadia, S.; Krishnan, B.; Wang, C.; Liebeskind, L. S. *J. Org. Chem.* **1994**, *59*, 5905−5911.
(18) Alcazar-Roman, L. M.; Hartwig, J. F. *Organometallics* **2002**, *21*, 491−502 and references therein.
(19) Two equivalents of bisphosphine per equivalent of $Pd(OAc)_2$ are required because 1 equiv of the bisphosphine is consumed in the reduction of Pd(II) to Pd(0). See: (a) Amatore, C.; Jutand, A.; Thuilliez, A. *Organometallics* **2001**, *20*, 3241−3249. (b) Ozawa, F.; Kubo, A.; Hayashi, T. *Chem. Lett.* **1992**, 2177−2180. (c) Amatore, C.; Carre, E.; Jutand, A.; M'Barki, M. A. *Organometallics* **1995**, *14*, 1818−1826.
(20) In all cases, the major epimer had the methyl or ethyl substituent in the β orientation, as depicted in the diagram accompanying Table 1.

Table 1. Asymmetric Palladacyclizations

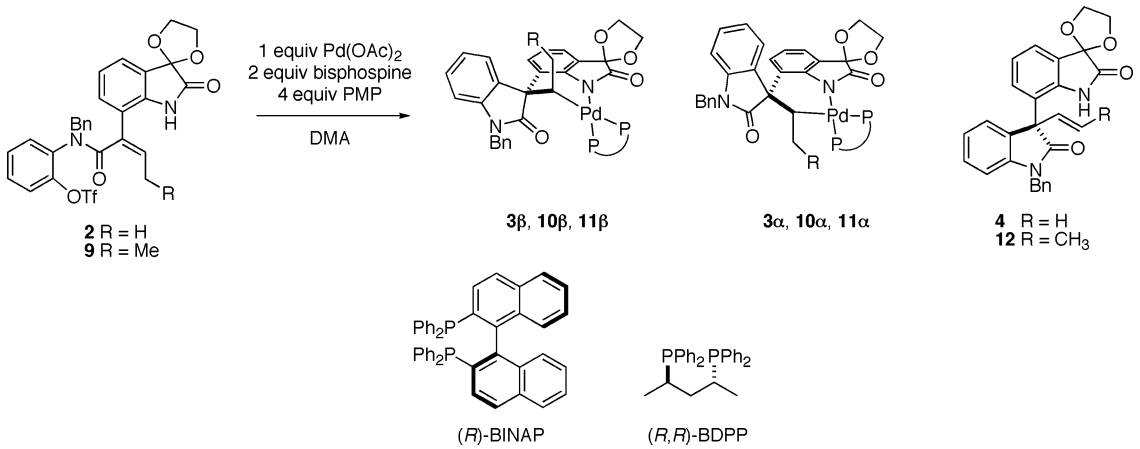

entry	aryl triflate	bisphosphine/[P–P]	temp, °C	R	palladacycle	yield,%[a]	dr[b,c]
1	**2**	(*R*)-BINAP	80	H	**3**	95[d]	96:4
2	**2**	(*S*)-BINAP	80	H	***ent*-3**	84[d]	93:7
3	**2**	(*R*,*R*)-BDPP	70	H	**10**	94[d]	96:4
4	**2**	(*S*,*S*)-BDPP	70	H	***ent*-10**	89[d]	95:5
5	**9**	(*R*)-BINAP	80	Me	**11**	67[e]	94:6

[a] Yield refers to the isolated yield after chromatography. [b] In all cases, diastereomeric ratios were determined by $^{31}P\{^1H\}$ NMR analysis of the crude product mixtures. [c] The diastereomeric ratios are written as the ratio of the β:α methyl (or ethyl) epimers as assigned by X-ray crystallography and/or NMR analysis. [d] The product of β-H elimination (**4**) was not detected in the ^1H NMR of the crude reaction mixture. [e] Heck product **12** was isolated in 17% yield and a 97:3 er (93% ee).

and achiral phosphine ligands[22] were evaluated under similar conditions, but only trace amounts (if any) of the corresponding palladacycles were detected by $^{31}P\{^1H\}$ NMR analysis of the crude reaction mixtures.

The structure of palladacycle **3*β*** was assigned initially on the basis of mass spectrometric and NMR spectroscopic evidence.[8] The electrospray mass spectrum of **3*β*** showed the characteristic palladium isotope pattern. Two-dimensional $^{31}P-^1H$ correlation and ^{31}P-decoupled ^1H NMR experiments proved the existence of the $-CH(CH_3)Pd$ fragment of palladacycle **3*β***. A chemical shift of 43.7 ppm in the ^{13}C NMR spectrum is typical of sp^3-hybridized carbons bonded to palladium; a doublet of doublets splitting pattern is consistent with coupling to two phosphorus atoms.

In the $^{13}C\{^1H\}$ NMR spectrum of **10*β***, the carbonyl carbon C12 (180.19 ppm, THF-d_8) of the *N*-benzyloxindole substituent, distinguished by ^{17}O-labeling studies that will be described later in this report, appears as a doublet of doublets (J = 2.4, 0.5 Hz) because of coupling to the two phosphorus atoms. Variable temperature $^{13}C\{^1H\}$ NMR studies from −80° to +80 °C revealed no change in either the chemical shift or coupling constants of C12. Similar diagnostic signals are observed in the $^{13}C\{^1H\}$ NMR spectra of palladacycles **3*β*** and **11*β***. The *N*-benzyloxindole carbonyl carbon C12 of palladacycle **3*β*** (181.79 ppm, THF-d_8) exhibits a small coupling to one of the two phosphorus atoms with a J-value of 1.8 Hz, and the oxindole carbon in **11*β*** is a doublet at 180.38 ppm with a 2.8 Hz coupling constant.

The infrared absorptions of the carbonyl groups of the palladacyclic complexes shown in Table 1 provide useful structural information about these complexes and their products (see below). Precursors **2** and **9** exhibit stretches at 1729 and 1733 cm^{-1} belonging to the isatin carbonyl groups. These absorptions of the corresponding Heck products **4** and **12** are seen at 1741 cm^{-1} for both compounds, with the oxindole carbonyl stretches appearing at 1695 and 1698 cm^{-1}, respectively. In the six-membered palladacycles, the absorption of the isatin acetal carbonyl group is shifted to much lower wavenumber; the carbonyl signals of the palladacyclic complexes are: **3*β*** − 1695 (oxindole carbonyl) and 1668 (isatin acetal) cm^{-1}, **10*β*** − 1698 and 1671 cm^{-1}, and **11*β*** − 1692 and 1677 cm^{-1}. The assignments of the carbonyl IR absorptions of **3*β***, **10*β***, **4**, and products derived from **3*β*** and **10*β*** were rigorously assigned by ^{17}O labeling (see later discussion).

X-ray Crystallography. The structures of palladacycles **10*β*** and **3α** were confirmed by X-ray crystallography. Palladacycles **3**, **10**, and **11** were isolated initially as powders, but single crystals of palladacycle **10*β*** suitable for an X-ray diffraction study were grown from a diethyl ether solution.[23] Figure 1 shows the solid-state structure of **10*β***.[24] The structure was solved in

(21) HPLC analyses [(Daicel Chiracel OD-H column, column temperature 45 °C, *n*-hexane-2-propanol = 96:4, flow rate = 0.5 mL·min^{-1}): 65.8 min (minor enantiomer), 74.3 (major enantiomer)] to determine enantiomeric purity were calibrated with samples of the corresponding racemate.

(22) The list of phosphine ligands includes: triphenylphosphine (PPh_3), 1,2-bis(dimethylphosphino)ethane (DMPE), 1,2-bis(diphenylphosphino)ethane (DPPE or DIPHOS), 1,3-bis(diphenylphosphino)propane (DPPP), 1,4-bis(diphenylphosphino)butane (DPPB), 1,2-bis(dicyclohexylphosphino)ethane, 1,1′-bis(diphenylphosphino)ferrocene (DPPF), 9,9-dimethyl-4,5-bis(diphenylphosphino)xanthene (XANTPHOS), bis(2-diphenylphosphinophenyl)-ether (DPEphos), (2S,3S)-(−)-bis(diphenylphosphino)butane [(*S*,*S*)-CHIRAPHOS], (4*R*,5*R*)-(−)-*O*-isopropylidene-2,3-dihydroxy-1,4-bis(diphenylphospino) butane [(*R*,*R*)-DIOP], (4*S*,5*S*)-(+)-*O*-isopropylidene-2,3-dihydroxy-1,4-bis(diphenylphospino) butane [(*S*,*S*)-DIOP], *R*-(+)-1,2-bis(diphenylphosphino)propane [(*R*)-PROPHOS], (*R*)-(+)-2-[2-(diphenylphosphino)-phenyl]-4-(1-methylethyl)-4,5-dihydrooxazole, (*S*)-(−)-2-[2-(diphenylphosphino)phenyl]-4-(1-methylethyl)-4,5-dihydrooxazole, (*R*)-(+)-2, 2′-bis(di-*p*-tolylphosphino)-1,1′-binaphthyl [(*R*)-Tol-BINAP], (*S*)-(−)-2,2′-bis(dicyclohexylphosphino)-1,1′-binaphthyl [(*S*)-Cy-BINAP].

(23) A single-crystal X-ray crystal structure of **10*β*** was also obtained from crystals grown by slow diffusion of cyclohexane into THF. In this case, the diffraction symmetry was 2/*m* and the systematic absences were consistent with the centrosymmetric monoclinic space group $P2_1/n$ that is indicative of a racemic crystal. Presumably in this solvent the small amount of racemate [<1% based on the ee of the (*R*,*R*)-BDPP ligand] employed for the palladacyclization was deposited.

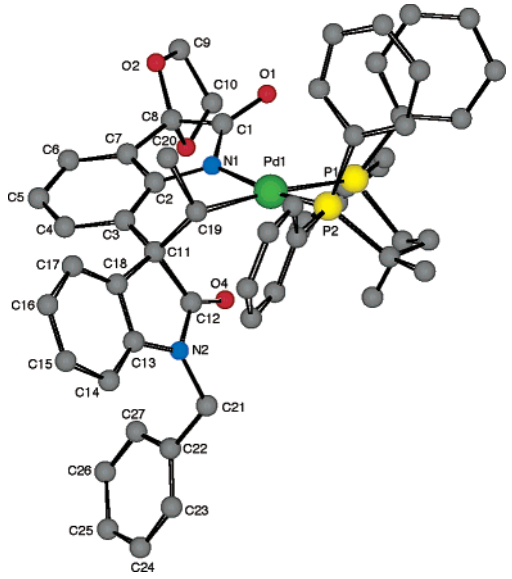

Figure 1. Solid-state structure of palladacycle **10*β***. Hydrogen atoms have been omitted for clarity.

the monoclinic, noncentrosymmetric space group $P2_1$. The absolute configuration of the quaternary center is *R*, in accord with earlier findings from this group.[25] The Pd−N bond length of 2.073 Å is within the range observed for other group 10 M−N single bonds (2.019−2.184 Å).[26] The P1−Pd−P2 bond angle is 89.4°. The Pd−P bond lengths differ by 0.121 Å (Pd−P1 = 2.393 Å; Pd−P2 = 2.272 Å), with the longer being trans to the strong trans-effecting alkyl ligand.[27] Oxygen O4 of the *N*-benzyloxindole substituent is positioned below the Pd atom at a distance of 2.966 Å. Although this distance is too long for a bonding interaction (Pd−O bonds are on the order of 2.1−2.2 Å[28]), it is within the sum of the van der Waals radii (3.10 Å) of the atoms concerned.[29] Square planar complexes of Pd(II) commonly form weak axial bonding interactions with hydrogen,[30] nitrogen,[31] and sulfur[32] atoms; a few examples of axial Pd−O interactions have also been reported, with Pd−O distances of 2.653−3.084 Å.[33,34] Despite this weak bonding interaction with O4, the ligand arrangement about the metal center of **10*β*** remains nearly square planar; the Pd atom lies 0.032 Å below the least-squares plane containing P1, P2, C19, and N1.

The X-ray crystal structure of **10*β*** reveals a flattened chair, or sofa, conformation for the six-membered palladacyclic ring, with five of the six atoms of the ring being nearly coplanar: the dihedral angles defined by Pd−N1−C2−C3 and C11−C3−C2−N1 are 0.0° and 4.1°, respectively. The out-of-plane carbon bonded to Pd, C19, forms dihedral angles of 42.4° and 22.6° with C11−C3−C2 and Pd−N1−C2, respectively. In this solid-state structure, the methyl group is oriented perpendicularly to the palladacyclic ring.

In the BINAP palladacycle series, crystals of the minor diastereomer **3α** suitable for X-ray diffraction analysis were grown from a methanol solution. This structure, shown in Figure 2, was also solved in the $P2_1$ space group.[35] Again the absolute configuration of the quaternary carbon is *R*. The Pd−N1 bond length of 2.040 Å is similar to the Pd−N1 distance observed in the X-ray crystal structure of **10*β***. The P1−Pd−P2 bond angle is 94.3°, within the range of bite angles for BINAP complexes of the nickel triad (90.8−95.8°).[18] The Pd−P bond lengths differ by 0.124 Å (Pd−P1 = 2.400 Å; Pd−P2 = 2.276 Å), with the longer bond again being trans to the alkyl ligand.[27] The six-membered palladacyclic ring of **3α** is in a sofa conformation, as in the solid-state structure of **10*β***, but in the ring-flipped conformation. The dihedral angle defined by Pd1−N1−C2−C3 is 1.2°, whereas a 5.3° dihedral angle is observed between C11−C3−C2−N1. The out-of-plane secondary carbon, C19, forms 32.3° and 27.0° dihedral angles with C11−C3−C2 and Pd−N1−C2, respectively. In the solid state, the α-methyl group also is oriented perpendicularly to the palladacyclic ring. In this epimer, the methyl hydrogens are in the shielding cones of the π-bond of the *N*-benzyloxindole carbonyl group and one of the phenyl rings of the (*R*)-BINAP ligand accounting for the unusual upfield chemical shift observed for this methyl group in the ^{1}H NMR spectrum (0.00 ppm in $CDCl_3$).

Thermal Stability of Palladacycle 3*β*. The thermal stability of palladacycle **3*β*** in solvents of varying polarity was investigated. Heating **3*β*** in toluene or mesitylene at temperatures ranging from 100 to 140 °C brought about slow *β*-hydride elimination to give Heck product **4** (obtained in ∼10−60% yield, by NMR analysis) together with several additional unidentified products. However, upon heating **3*β*** in anhydrous DMF or DMA[36] at 140 °C, a new palladacyclic product was observed by ^{1}H and ^{31}P{^{1}H} NMR analysis (Table 2).[37] Isolation of this product (in 10−15% yield) allowed its unambiguous

(24) Crystallographic data for this compound were deposited at the Cambridge Crystallographic Data Centre: CCDC 247401.
(25) Reference 15 and unpublished results from the Overman laboratories.
(26) The CCDC was searched for first-order M−N (M = Ni, Pd, Pt) bonding distances of four-coordinate complexes with similar ligand composition.
(27) (a) Kakino, R.; Nagayama, K.; Shimizu, I.; Yamamoto, A. *Chem. Lett.* **1999**, 685−686. (b) Owen, G. R.; Vilar, R.; White, A. J. P.; Williams, D. J. *Organometallics* **2003**, *22*, 4511−4521.
(28) Orpen, A. G.; Brammer, L.; Allen, F. H.; Kennard, O.; Watson, D. G.; Taylor, R. *J. Chem. Soc., Dalton Trans.* **1989**, *12*, S1−S83.
(29) Huheey, J. E.; Keiter, E. A.; Keiter, R. L. *Inorganic Chemistry; Principles of Structure and Reactivity*, 4th ed.; Harper Collins: New York, 1993; Table 8.1, p 292.
(30) (a) Albinati, A.; Anklin, C. G.; Ganazzoli, F.; Rüegg, H.; Pregosin, P. S. *Inorg. Chem.* **1987**, *26*, 503−508. (b) Albinati, A.; Pregosin, P. S.; Wombacher, F. *Inorg. Chem.* **1990**, *29*, 1812−1817. (c) Albinati, A.; Lianza, F.; Pregosin, P. S.; Müeller, B. *Inorg. Chem.* **1994**, *33*, 2522−2526. (d) Casas, J. M.; Falvello, L. R.; Forniés, J.; Martín, A.; Welch, A. J. *Inorg. Chem.* **1996**, *35*, 6009−6014. (e) Stambuli, J. P.; Incarvito, C. D.; Bühl, M.; Hartwig, J. F. *J. Am. Chem. Soc.* **2004**, *126*, 1184−1194.
(31) Hunter, G.; McAuley, A.; Whitcombe, T. W. *Inorg. Chem.* **1988**, *27*, 2634−2639.
(32) (a) Blake, A. J.; Holder, A. J.; Hyde, T. I.; Roberts, Y. V.; Lavery, A. J.; Schröder, M. *J. Organomet. Chem.* **1987**, *323*, 261−270. (b) Blake, A. J.; Gilby, L. M.; Gould, R. O.; Lippolis, V.; Parsons, S.; Schröder, M. *Acta Crystallogr.* **1988**, *C54*, 295−298. (c) Grant, G. J.; Sanders, K. A.; Setzer, W. N.; VanDerveer, D. G. *Inorg. Chem.* **1991**, *30*, 4053−4056. (d) Chandrasekhar, S.; McAuley, A. *Inorg. Chem.* **1992**, *31*, 2663−2665. (e) Lucas, C. R.; Liu, S. *Inorg. Chim. Acta* **1995**, *230*, 133−138. (f) Chak, B.; McAuley, A.; Whitcombe, T. W. *Inorg. Chim. Acta* **1996**, *246*, 349−360. (g) Lee, G.-H.; Tzeng, B.-C. *Acta Crystallogr.* **1996**, *C52*, 879−882.
(33) (a) Louis, P. R.; Pelissard, D.; Weiss, R. *Acta Crystallogr.* **1974**, *B30*, 1889−1894. (b) Okeya, S.; Miyamoto, T.; Ooi, S.; Nakamura, Y.; Kawaguchi, S. *Inorg. Chim. Acta* **1980**, *45*, L135−L137. (c) Siedle, A. R.; Pignolet, L. H.; Newmark, R. A. *J. Am. Chem. Soc.* **1981**, *103*, 4947−4948. (d) Lucas, C. R.; Liang, W.; Miller, D. O.; Bridson, J. N. *Inorg. Chem.* **1997**, *36*, 4508−4513. (e) Park, K.-M.; Yoon, I.; Yoo, B. S.; Choi, J. B.; Lee, S. S.; Kim, B. G. *Acta Crystallogr.* **2000**, *C56*, 1191−1192.
(34) The observed distance between Pd and O4 of **10*β*** is also in close agreement with axial Pd−O distances calculated by molecular modeling (2.944−2.974 Å). See: Park, J.-K.; Cho, Y.-G.; Lee, S. S.; Kim, B. G. *Bull. Korean Chem. Soc.* **2004**, *25*, 85−89.
(35) Crystallographic data for this compound were deposited at the Cambridge Crystallographic Data Centre: CCDC 247402.
(36) Anhydrous DMF was obtained by sparging with argon and then passing through a drying column made by Glass Contours, Inc. Anhydrous DMA was obtained by stirring DMA purchased from Acros over CaH_2 under argon overnight and distilling under reduced pressure into a flask having a Teflon seal.
(37) Slow conversion of **3*β*** to **3α** was seen also in DMSO, although unidentified decomposition products were the major products produced.

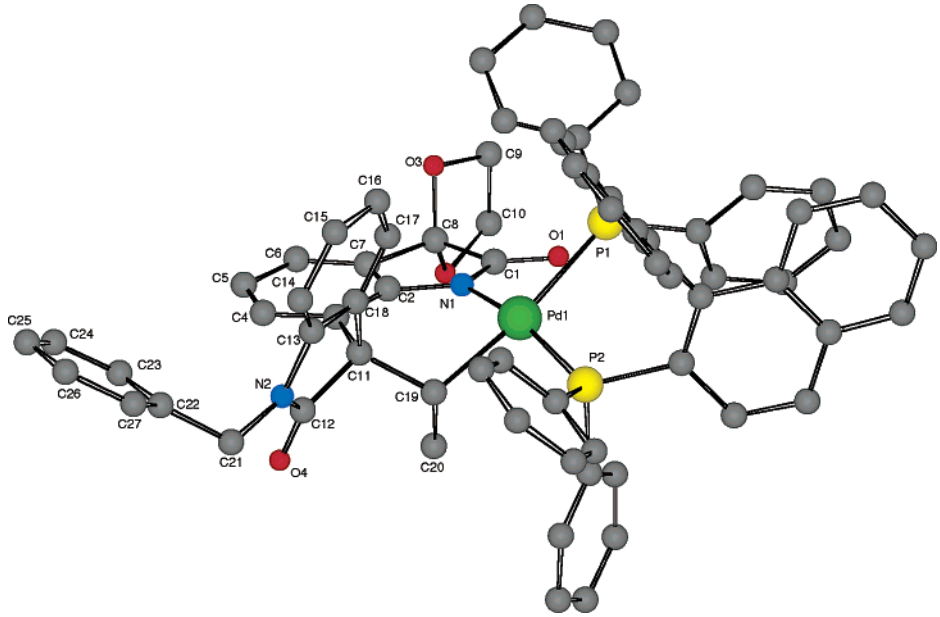

Figure 2. Solid-state structure of palladacycle **3α**. Hydrogen atoms have been omitted for clarity.

Table 2. Epimerization Studies of **3*β*** in DMF at 140 °C

entry	DMF	time (h)	**3*β***:**3α** ratio	**3α** yield, %[a]
1	anhydrous[b]	1	1.0:0.4	19
2	anhydrous[b]	2	1.0:0.6	21
3	anhydrous[b]	4	1.0:1.7	21
4	anhydrous[b]	5	1.0:2.7	22
5	anhydrous[b]	6	1.0:5.4	19
6	wet[c]	1	1.0:4.9	30
7	wet[c]	2	<1:20	27

[a] Yields were determined by integrating peaks in the $^{31}P\{^1H\}$ NMR spectrum versus an external standard of H_3PO_4-d_3. The remaining material was unidentified decomposition products. [b] Anhydrous DMF was obtained by sparging with argon and then passing through a drying column made by Glass Contours, Inc. [c] Wet DMF was obtained by adding 10 μL of water to 0.5 mL of anhydrous DMF.

identification as **3α**, the minor epimer produced in the original palladacyclization reaction. Particularly diagnostic are the doublets in the $^{31}P\{^1H\}$ NMR spectrum at 22.2 and 19.4 ppm and the signal at 0.00 ppm in the ^1H NMR spectrum for the methyl group.

To gain insight into the conversion of **3*β*** to **3α**, the latter was heated in THF at 80 °C with excess TBP·HOTf to occasion β-hydride elimination to produce Heck product **4**. Comparison of the enantiomeric excess of this material (96% ee) to that formed upon cleavage of palladacycle **3*β*** under similar conditions (93% ee) showed that no erosion of configuration at the quaternary center had occurred during epimerization of the methyl group.[38] Warming palladacycle **3α** to 140 °C in DMF for prolonged periods of time did not result in the formation of **3*β***, but rather gave rise to decomposition of **3α** to produce **4**, (*R*)-BINAP, (*R*)-BINAP[O], and other unidentified products.

The rate of epimerization of **3*β*** was markedly increased when it was heated in a solvent containing H_2O. For example, warming **3*β*** for 1 h at 140 °C in wet DMF (see footnote c, Table 2) provided a 5:1 mixture of α:β epimers (entry 6). After an additional hour at this temperature, diagnostic signals for

(38) The enantiomeric excess was measured by chiral HPLC using a Daicel Chiracel OD-H column (35 °C, 90:10 *n*-hexane:isopropanol, 1.0 mL/min) against a racemic sample.

Scheme 3. Acid-Promoted Epimerization of the Palladium−Carbon Stereocenter in Palladacycles **3*β*** and **10*β***

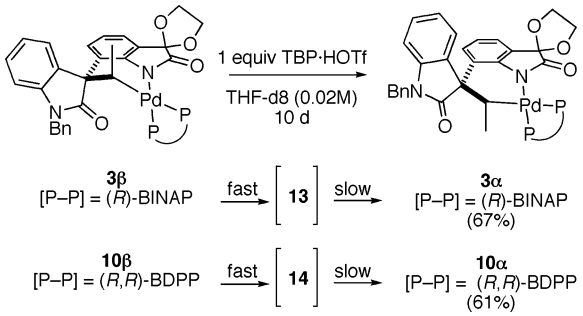

the β-methyl epimer are no longer seen in the $^{31}P\{^1H\}$ NMR spectrum (entry 7). Epimerization of the stereogenic palladium−carbon center also occurred in wet DMA (10 μL of water added to 0.5 mL of anhydrous DMA) at 140 °C at a similar rate to that observed in wet DMF.

Acid-Promoted Epimerization of 3*β* and Identification of New Palladium Complexes. Epimerization of the palladium−carbon stereocenter of **3*β*** and **10*β*** can be accomplished in higher yield under mildly acidic conditions. Maintaining a dilute solution of **3*β*** [$^{31}P\{^1H\}$ NMR in THF-d_8: δ 28.9 (d, ^2J(P−P) = 50.9 Hz), 18.5 (d, ^2J(P−P) = 52.2 Hz)] in THF (0.02 M) containing 1 equiv of TBP·HOTf at room temperature yielded 67% of palladacycle **3α** [$^{31}P\{^1H\}$ NMR in THF-d_8: δ 22.3 (d, ^2J(P−P) = 43.6 Hz), 19.3 (d, ^2J(P−P) = 43.6 Hz)] after 10 days (Scheme 3). Monitoring this reaction by $^{31}P\{^1H\}$ NMR revealed that an intermediate BINAP-bound palladium complex **13** [$^{31}P\{^1H\}$ NMR in THF-d_8: δ 41.9 (d, ^2J(P−P) = 49.5 Hz), 16.4 (d, ^2J(P−P) = 49.5 Hz)] formed rapidly upon addition of TBP·HOTf; this intermediate then slowly transformed to palladacycle **3α**. A related intermediate, BDPP-bound palladium complex **14** [$^{31}P\{^1H\}$ NMR in THF-d_8: δ 45.2 (d, ^2J(P−P) = 59.7 Hz), 9.5 (d, ^2J(P−P) = 59.6 Hz)], was observed when pure palladacycle **10*β*** [$^{31}P\{^1H\}$ NMR in THF-d_8: δ 28.3 (d, ^2J(P−P) = 57.6 Hz), 8.7 (d, ^2J(P−P) = 56.2 Hz)] was treated under similar conditions, yielding 61%[39] of palladacycle **10α**

Table 3. Conversion of **3*β*** to **13** upon Treatment with TBP·HOTf after ~5 min at Ambient Temperature

entry	[**3*β***] in THF, M	equiv TBP·HOTf	conversion to **13**, %[a]
1	0.02	0.2	17[b]
2	0.02	0.4	47[b]
3	0.02	0.8	83[b]
4	0.02	1.0	100
5	0.01	3.0	100

[a] Determined by $^{31}P\{^1H\}$ NMR analysis using an external standard of H_3PO_4-d_3. [b] The remaining material was unreacted starting palladacycle **3*β***.

[$^{31}P\{^1H\}$ NMR in THF-d_8: δ 33.3 (d, $^2J(P-P) = 52.2$ Hz), 20.1 (d, $^2J(P-P) = 52.2$ Hz)].

In an attempt to employ palladacycles **3** and **10** in C−C and C−heteroatom bond-forming reactions, palladacycle **3*β*** or **10*β*** was allowed to react with 1 equiv of TBP·HOTf in MeOH in the presence of 1 atm CO.[40] In each case, dioxindole propionic ester **15** was produced in high yield (eq 2). The formation of ester **15** from palladacycle **3*β*** under these conditions could be followed by $^{31}P\{^1H\}$ and ^1H NMR. Upon addition of TBP·HOTf, palladacycle **3*β*** was rapidly converted to intermediate **13**. No further palladium-containing intermediates were detected by $^{31}P\{^1H\}$ NMR and ^1H NMR analysis, while peaks for methyl ester **15** slowly began to grow in over time.[41]

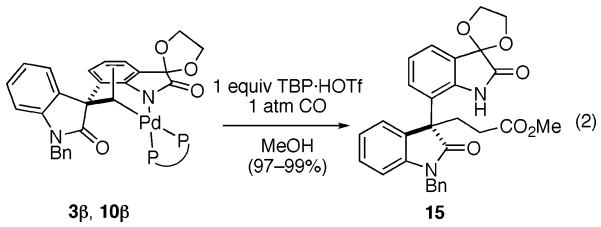

The precise conditions under which palladacycles **3*β*** and **10*β*** were allowed to react in the presence of the mild acid TBP·HOTf, in particular the palladacycle concentration and the number of equivalents of TBP·HOTf, affected the reaction outcome. When palladacycle **3*β*** (or **10*β***) was exposed in THF at ambient temperature to less than 1 equiv of TBP·HOTf, palladium complex **13** (or **14**) initially formed within 5 min in a proportion corresponding approximately to the amount of acid used. For example, adding 0.2 equiv of TBP·HOTf to a 0.02 M solution of **3*β*** in THF-d_8 resulted in 17% conversion to **13** as determined by $^{31}P\{^1H\}$ NMR analysis, whereas use of 0.4 equiv of TBP·HOTf produced 47% of **13** and 0.8 equiv of TBP·HOTf similarly led to the formation of **13** in 83% (Table 3). When **3*β*** was allowed to react with 1−3 equiv of TBP·HOTf, complete conversion to **13** in <5 min was observed by $^{31}P\{^1H\}$ NMR.

Additional characterization data for palladium complexes **13** and **14** were gathered to elucidate their structures. The ^1H NMR spectra of **13** and **14** lack signals for both the methyl group (0.89−1.07 ppm) and the methine hydrogen (1.49−1.59 ppm) that are indicative of palladium attached to a secondary carbon. Instead, these four hydrogens appear as discreet multiplets between 2.37 and 1.04 ppm in complexes **13** and **14**. Each of these four hydrogens in **13** and **14** is coupled to the other three hydrogens and to both phosphorus atoms.[42] These data are consistent with palladium bound to the terminus of a CH_2CH_2 fragment. The $^{31}P\{^1H\}$ NMR spectrum (in THF-d_8) of palladium complex **13** shows a pair of $J_{A,B}$ doublets at 41.9 and 16.4 ppm. The corresponding phosphorus signals for palladacycle **3*β*** are observed at 28.9 and 18.5 ppm, signifying that one phosphorus atom is significantly more deshielded in complex **13**. The $^{31}P\{^1H\}$ NMR spectrum (in THF-d_8) of palladium complex **14** contains a pair of $J_{A,B}$ doublets at 45.2 and 9.5 ppm; comparable signals for palladacycle **10*β*** occur at 28.3 and 8.7 ppm, signifying that again one phosphorus atom has become considerably more deshielded in complex **14** as well.[43]

The ESI-MS traces of **13** and **14** display a single cluster with the predicted palladium isotope pattern (**13**: $m/z = 1167$ for ^{106}Pd; **14**: $m/z = 985$ for ^{106}Pd). These masses correspond to those of the starting palladacycles **3*β*** and **10*β*** plus 1 amu, respectively. These data are consistent with these intermediates being neutral palladium complexes that are isomeric to **3*β*** or **10*β***, or cationic palladium complexes each having a mass one higher than that of the corresponding starting palladacycle. In the ^1H NMR spectra of **13** and **14**, it was unclear whether an N−H hydrogen was present because the aryl hydrogens of the phosphorus ligands obscure this region. To distinguish between these two possibilities and ascertain whether palladium remains bound to the oxindole nitrogen in palladium complexes **13** and **14**, ^{15}N-labeled analogues were prepared.

Synthesis of ^{15}N-Labeled Palladacycles and Their Evaluation by ^{15}N NMR. The ^{15}N-labeled palladacycle precursor **[^{15}N]2** was constructed in seven steps from 98% ^{15}N-labeled aniline **16** (Scheme 4). Protection of ^{15}N-aniline with a BOC group initially provided **17**. Subsequent BOC-directed ortholithiation and quenching of the aryllithium intermediate with diiodoethane delivered aryl iodide **18**. Acid-mediated deprotection of crude **18** afforded ^{15}N-2-iodoaniline (**19**) in good overall yield from ^{15}N-aniline. Following a standard procedure,[44] ^{15}N-2-iodoaniline (**19**) was allowed to react with chloral hydrate and NH_2OH·HCl to give **20**, which was cyclized to give isatin **21**. Ketalization of **21** provided **[^{15}N]8**. Stille coupling of this intermediate with vinyl stannane **22** completed the synthesis of ^{15}N-labeled palladacyclization precursor **[^{15}N]2**. Palladacyclization of aryl triflate **[^{15}N]2** by the procedures described earlier gave ^{15}N-labeled palladacycles **[^{15}N]3*β*** and **[^{15}N]10*β***.

Consistent with the isatin acetal being ligated to palladium at nitrogen, six-membered palladacycles **[^{15}N]3*β*** and **[^{15}N]10*β*** exhibit reciprocal splitting between ^{15}N and ^{31}P. In both the ^{15}N and $^{15}N\{^1H\}$ NMR spectra of **[^{15}N]3*β***, a doublet of doublets centered at −232.8 ppm appears as a result of the two-bond coupling with the two phosphorus atoms (Table 4). A doublet

(39) Yield was determined by $^{31}P\{^1H\}$ NMR integration versus an external standard of H_3PO_4-d_3 (solution in H_2O). Palladacycle **10α** was not isolated.
(40) Direct carbonylation of **3*β*** or **10*β*** with CO and MeOH to give a secondary methyl ester product did not occur under forcing conditions (high temperature). The use of the additive $AgBF_4$ caused *β*-hydride elimination to **4**.
(41) Monitoring the reaction of palladacycle **11*β*** (as a 94:6 mixture of *β*:α methyl epimers) and 1 equiv of TBP·HOTf in THF-d_8 by $^{31}P\{^1H\}$ NMR revealed a complex product mixture displaying a pair of diagnostic doublets at δ 30.2 (d, $J(P-P) = 64.4$ Hz) and 6.2 (d, $J(P-P) = 64.4$ Hz). Attempts to isolate this product were unsuccessful. Reactions of palladacycle **11*β*** with various amounts of TBP·HOTf in a CO-saturated solution of MeOH resulted in *β*-hydride elimination to give Heck product **12**; no evidence of the formation of methyl ester analogues of **15** was seen in these reactions.
(42) The $^3J(P-H)$ and $^5J(P-H)$ coupling constants of these multiplets were deduced by ^1H NMR experiments with selective ^{31}P decoupling using low power continuous wave decoupling of the individual multiplets.
(43) Palladacycle **14** decomposed during attempted isolation; thus, it was characterized in situ in THF-d_8. The inability to isolate palladacycle **14** is likely attributable to the less bulky BDPP ligand.
(44) Lisowski, V.; Robba, M.; Rault, S. *J. Org. Chem.* **2000**, *65*, 4193−4194.

Scheme 4 [a]

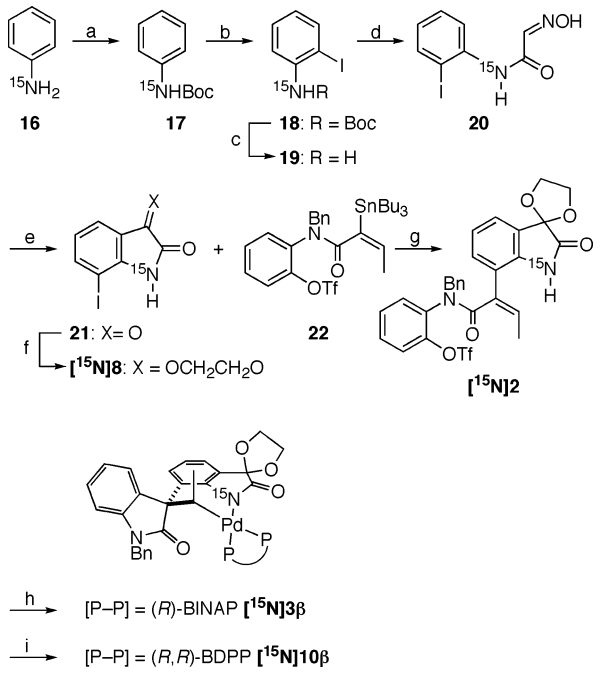

[a] Conditions: (a) Boc_2O, THF, 0 °C to room temperature (98%); (b) *t*-BuLi, diiodoethane, Et_2O, −78 to −25 °C; (c) 1:1 HCl:EtOAc (65% over two steps); (d) chloral hydrate, $Na_2SO_4 \cdot 10H_2O$, $NH_2OH \cdot HCl$, HCl, H_2O, 90°C (97%); (e) H_2SO_4, 50−80 °C (82%); (f) ethylene glycol, $TsOH \cdot H_2O$, benzene, 80 °C (85%); (g) 10 mol % $Pd_2dba_3 \cdot CHCl_3$, 60 mol % P(2-furyl)$_3$, 2 equiv of CuI, NMP (53%); (h) 1 equiv of $Pd(OAc)_2$, 2 equiv of (*R*)-BINAP, 4 equiv of PMP, DMA, 80 °C; (i) 1 equiv of $Pd(OAc)_2$, 2 equiv of (*R*,*R*)-BDPP, 4 equiv of PMP, DMA, 80 °C.

Table 4. $^{15}N\{^1H\}$ and ^{15}N NMR Multiplicities (m), Chemical Shifts (δ), and Coupling Constants (J) for [^{15}N]-Labeled Palladacycles

		$^{15}N\{^1H\}$ NMR		^{15}N NMR	
entry	δ, ppm	m	J, Hz	m	J, Hz
[15N]3*β*	−232.8	dd	^2J(N−P) = 39.1, 4.1	dd	^2J(N−P) = 39.1, 4.1
[15N]10*β*	−228.6	dd	^2J(N−P) = 40.5, 5.1	dd	^2J(N−P) = 40.5, 5.1
[15N]13	−255.4	s	−	d	^1J(N−H) = 95.2
[15N]14	−253.6	s	−	d	^1J(N−H) = 95.6

of doublets at −228.6 ppm is seen in ^{15}N and $^{15}N\{^1H\}$ NMR spectra of **[15N]10*β***.

Independent treatment of six-membered palladacycles **[15N]-3*β*** and **[15N]10*β*** with 1−3 equiv of TBP·HOTf in THF-d_8 resulted in their rapid and quantitative conversion to ^{15}N-labeled palladium complexes **[15N]13** and **[15N]14**, respectively.[45] The $^{15}N\{^1H\}$ spectra of **[15N]13** shows a singlet at −252.7 ppm, whereas the ^1H coupled ^{15}N spectra display a doublet (^1J(N−H) = 96.3 Hz) whose coupling constant is indicative of a one-bond N−H coupling.[46] Similarly, the $^{15}N\{^1H\}$ spectra of **[15N]14** show a singlet at −253.6 ppm, while the ^1H coupled ^{15}N spectra show a doublet (^1J(N−H) = 95.6 Hz). These data prove that the Pd−N bond is no longer intact in palladium complexes **13** and **14**. In light of these findings, we turned to investigate the possibility that the carbonyl group of the *N*-benzyloxindole substituent was bound to palladium in complexes **13** and **14**. Toward this end, the preparation of an ^{17}O-enriched analogue of precursor **2** was developed.

(45) The conversions of **[15N]3*β*** to **[15N]13** and **[15N]10*β*** to **[15N]14** were monitored by ^{31}P NMR with an internal standard to confirm that they were quantitative.

(46) Berger, S.; Braun, S.; Kalinowski, H.-O. *NMR Spectroscopy of the Non-Metallic Elements*; John Wiley & Sons: Chichester, U.K., 1997.

Synthesis of ^{17}O-Labeled Palladacycles. The low natural abundance of the NMR-active oxygen isotope ^{17}O and its high cost in enriched forms made late-stage incorporation of ^{17}O into the synthesis of ^{17}O-labeled **2** desirable. However, all efforts to install the ^{17}O label in an efficient and reliable manner late in the sequence were unsuccessful. Thus, a practical synthesis of **[17O]2** from 2-chlorobenzooxazole **23** and 70% enriched $H_2{}^{17}O$ was developed that delivered the ^{17}O-labeled palladacyclization precursor in five steps (Scheme 5). This sequence begins by hydrolysis of chlorobenzooxazole **23** in a diethyl ether solution of dry HCl in the presence of 1 equiv of 70% ^{17}O-labeled H_2O to give oxazolidinone **24** in near quantitative yield. After affixing a benzyl protecting group to **24**, addition of **[17O]5** to 1-propynyllithium at −78 °C in THF and quenching the resulting intermediate with *N*-phenyltriflimide provided **25** in 52% overall yield (97% based on recovered starting material, which could be recycled). Hydrostannylation of **25** proceeded in good yield to deliver **[17O]22**, which was coupled under Stille conditions with aryl iodide **8** to provide the desired palladacyclization precursor **[17O]2** in 56% yield. With **[17O]2** in hand, construction of the corresponding ^{17}O-labeled analogues of palladacycles **3** and **10** (**[17O]3*β*** and **[17O]10*β***) ensued as before.

Direct observation of the ^{17}O NMR spectra of the pertinent ^{17}O-labeled palladacycles was attempted, but the large quadrupole moment and the associated broad line widths of the ^{17}O nucleus hindered these efforts. However, the proximity of natural abundance ^{13}C to the incorporated ^{17}O label allowed the NMR active oxygen label to aid in the structural assignment of palladium complexes **13** and **14**. The nuclear spin of ^{17}O (5/2) provides a means to distinguish between the two carbonyl carbons in palladium complexes **13** and **14** as the carbon attached to the ^{17}O label appears as a broadened multiplet. Following the reactions of neutral palladacycles **[17O]3*β*** and **[17O]10*β*** with TBP·HOTf to form, respectively, **[17O]13** and **[17O]14** by $^{13}C\{^1H\}$ NMR revealed two trends: in the products, the oxindole carbonyl carbons are shifted downfield by 3.88 and 4.02 ppm, respectively, and the isatin acetal carbonyl carbons are shifted upfield by 5.83 and 4.91 ppm (Table 5, Figure 3). These ^{13}C NMR shifts evidence that the *N*-benzyloxindole fragment has lost electron density in palladium complexes **13** and **14**, suggesting the establishment of a new, weak bonding interaction between the carbonyl group of this group and the electron-poor palladium center.[47,48]

Further evidence to support ligation of the *N*-benzyloxindole fragment comes from infrared spectra of the relevant ^{17}O-labeled compounds. Comparison of the spectra of ^{17}O-labeled and unlabeled compounds allowed the carbonyl stretches to be unambiguously assigned to the oxindole or isatin functional groups in these molecules. In the IR spectrum of **[17O]3*β***, the carbonyl stretches appear together in a single broad band at 1670 cm^{-1} compared to the discrete stretches observed at 1696 and 1670 cm^{-1} in the spectrum of unlabeled **3*β***. The peak at 1696 cm^{-1} is assigned to the *N*-benzyloxindole carbonyl in palladacycle **3*β*** because of the unmistakable isotope shift it exhibits. Similarly, the carbonyl stretches at 1697 and 1670 cm^{-1} in the spectrum of unlabeled **10*β*** become a single broad peak at 1671 in the spectrum of **[17O]10*β***.

The infrared spectra displayed by ^{17}O-labeled and unlabeled palladium complexes **13** and **14** provided valuable information about their structures. The two carbonyl stretches in the IR

spectrum of Pd·BINAP complex **13** appear at 1746 and 1637 cm^{-1}. The high-frequency stretch is assigned to the isatin acetal carbonyl, because the IR spectrum of **[^{17}O]13** displays a peak at the same frequency (1745 cm^{-1}). The lower frequency stretch of the *N*-benzyloxindole carbonyl exhibits a clear isotopic shift, appearing at 1618 cm^{-1} in the IR spectrum of **[^{17}O]13**. A similar trend is observed in Pd·BDPP complex **14**: the higher frequency isatin acetal carbonyl shift (1741 cm^{-1}) is seen at the same frequency in **[^{17}O]14**. The lower frequency carbonyl shift observed for **14** (1618 cm^{-1}) is seen at 1605 cm^{-1} in the IR spectrum of **[^{17}O]14**, again linking this absorption to the oxindole carbonyl group. The assignment of the carbonyl stretch at 1741 cm^{-1} in the IR spectrum in Heck product **4** to the isatin carbonyl was confirmed by the presence of a peak at the same frequency in the IR spectrum of **[^{17}O]4**. The isotopic shift of the peak at 1695 cm^{-1} to 1677 cm^{-1} in the IR spectrum of **[^{17}O]4** confirmed its assignment to the oxindole carbonyl stretch. This absorption at 1741 cm^{-1} correlates well to the stretches assigned to the unbound isatin acetal carbonyl groups in complexes **13** and **14**. The observed stretches for the oxindole carbonyl groups of palladium complexes **13** and **14**, however, are shifted to lower wavenumber, indicating that these bonds are weakened by complexation to palladium.

Isolation of BINAP Complex 13 and Observation of Transient Pd·BINAP Intermediate 27. Although attempts to isolate BDPP complex **14** were fruitless, the BINAP complex **13** could be obtained in pure form. Treatment of palladacycle **3*β*** at ambient temperature in THF with excess trifluoroacetic acid (TFA) for 15 min, followed by azeotropic removal of residual TFA with heptane, gave a mixture of the desired palladium complex **13** and β-hydride elimination product **4**. After removal of **4** by washing this mixture with a small amount of diethyl ether, pure **13** was isolated as a powder in 37% yield.[49]

Scheme 5 [a]

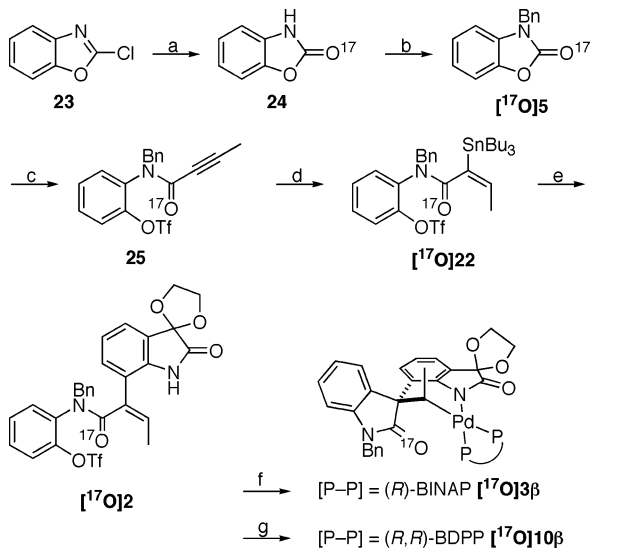

[a] Conditions: (a) 1 M HCl in Et_2O, 1 equiv of 70% $H_2{}^{17}O$ (99%); (b) BnCl, K_2CO_3, DMF, 125 °C (99%); (c) *n*-BuLi, BrCH=CHMe, THF, −78 to −25 °C, then $PhNTf_2$ (52%, 97% based on recovered **[^{17}O]5**); (d) 3 mol % $Pd(PPh_3)_4$, $HSnBu_3$ (78%); (e) **8**, 10 mol % Pd_2dba_3·$CHCl_3$, P(2-furyl)$_3$, CuI, NMP (56%); (f) 1 equiv of $Pd(OAc)_2$, 2 equiv of (*R*)-BINAP, 4 equiv of PMP, DMA, 80 °C; (g) 1 equiv of $Pd(OAc)_2$, 2 equiv of (*R*,*R*)-BDPP, 4 equiv of PMP, DMA, 80 °C.

Table 5. Carbonyl $^{13}C\{^1H\}$ NMR Shifts (δ), Multiplicities (m), and Coupling Constants (*J*) for **3*β***, **13**, **10*β***, and **14** in THF-d_8

		$^{13}C\{^1H\}$		
entry	carbonyl	m	δ CO, ppm	*J*, Hz[a]
3*β*	isatin	dd	182.16	$^3J(C-P) = 2.4, 0.9$
	oxindole	d	181.79	$^4J(C-P) = 1.8$
13	oxindole	m	185.67	−
	isatin	s	176.33	−
10*β*	oxindole	dd	180.19	$^4J(C-P) = 2.4, 0.5$
	isatin	dd	179.89	$^3J(C-P) = 3.8, 0.7$
14	oxindole	m	184.21	−
	isatin	s	174.98	−

[a] Coupling constants (*J*-values) were calculated with line broadening = 0.

With a reliable method to isolate BINAP complex **13** in hand, investigations of its transformation into Heck product **4** were undertaken. Addition of 1 equiv of TBP·HOTf to BINAP complex **13** in THF-d_8 resulted in the formation of a transient BINAP-bound palladium intermediate **27**, which then rapidly decomposed to Heck product **4** as observed by $^{31}P\{^1H\}$ and ^1H NMR analysis. Performing this transformation at reduced temperature extended the lifetime of intermediate **27**, allowing additional spectroscopic information to be obtained. At a probe temperature of −35 °C, reasonable ^1H, $^{13}C\{^1H\}$, $^{31}P\{^1H\}$, and COSY NMR spectra of complex **27** in THF-d_8 were collected. Although many peaks in the ^1H and $^{13}C\{^1H\}$ NMR spectra were

(47) Intensive NMR studies were undertaken to prove that the multiplets assigned to the *N*-benzyl oxindole carbonyl carbons in the $^{13}C\{^1H\}$ NMR spectra of palladium complexes **13** and **14** are attributable to long-range coupling to the two phosphorus atoms in each complex. A $^{13}C\{^1H\}$ NMR experiment with broadband ^{31}P decoupling was attempted; however, the large peak separation (~36−42 ppm) of the two phosphorus atoms in complexes **13** and **14** hampered these efforts as prohibitively high power levels were required to effectively decouple both phosphorus atoms. Attempts to selectively irradiate at each ^{31}P frequency while observing the carbonyl region of the $^{13}C\{^1H\}$ NMR spectrum also gave somewhat ambiguous results, although some simplification and increase in relative peak heights of the *N*-benzyl oxindole carbonyl carbons was observed in the $^{13}C\{^1H\}$ NMR spectra of **13** and **14**. A $^{13}C\{^1H\}$ experiment employing sculpted-pulse ^{31}P decoupling, which in theory provides the required high decoupling power centered at the phosphorus atom frequencies and none between, also fell short of fully decoupling phosphorus in complexes **13** and **14**. The difficulties associated with effectively decoupling ^{31}P while observing ^{13}C led to two additional NMR experiments being attempted. A ^{31}P isotope selection and a $^{31}P-^{13}C$ INEPT, designed to output a 1D ^{13}C NMR spectra containing only the carbons that are coupled to phosphorus, did not reveal the desired $^{13}C-^{31}P$ correlation. One possible explanation for their failure is that the small *J*-values of the multiplets (several ~1−2 Hz coupling constants) undermined these two NMR experiments because of a (1/*J*·n) ms acquisition delay embedded in their pulse sequences. Consequently, optimizing such an NMR experiment for complexes **13** and **14** using an approximate *J* value of 2 Hz translates to a 250 ms acquisition delay (when $n = 2$) during which time a significant amount of signal is lost because of relaxation. Although quaternary carbons typically have long relaxation times, manipulation of ^{13}C data collected without an acquisition delay suggests that the first 250 ms represents a large portion of the total signal. So although the most probable explanation for the complex *N*-benzyl oxindole carbonyl ^{13}C peaks of palladium complexes **13** and **14** is through-bond coupling to the two phosphorus atoms, we have thus far been unable to rigorously prove this correlation.

(48) In attempts to grow X-ray quality crystals of **13** and **14** for structural characterization, the transformations of **3*β*** to **13** and **10*β*** to **14** were also performed with the TBP·H salts with PF_6, BF_4, BPh_4, TFA, and Cl counteranions. Single crystals were not obtained. The $^{31}P\{^1H\}$ NMR spectra of **13** and **14** obtained with these counterions matched those from TBP·HOTf.

(49) Complex **13** was not stable to silica gel chromatography; eluting with ether/hexanes on a column of Merck silica gel resulted in complete decomposition, whereas switching to Davisil (a silicotungstic acid hydrate sorbent that is commercially available from Fisher) provided an eluent that was an inseparable 2:1 mixture of complex **13** and an unidentified BINAP-bound palladium complex **26**. Complex **26** could not be isolated in pure form. However, spectroscopic evidence obtained from the mixture of **13** and **26** showed that the latter also has two methylene carbons that are each split by two phosphorus atoms. Furthermore, evidence of an N−H bond is seen in ^{15}N NMR spectra of **26**. When the mixture of **13** and **26** was exposed to 1 equiv of TBP·HOTf, both led to Heck product **4**. To circumvent the undesired formation of **26**, a volatile acid was employed to transform palladacycle **3*β*** to **13**, thus obviating the need for purification of the product by column chromatography.

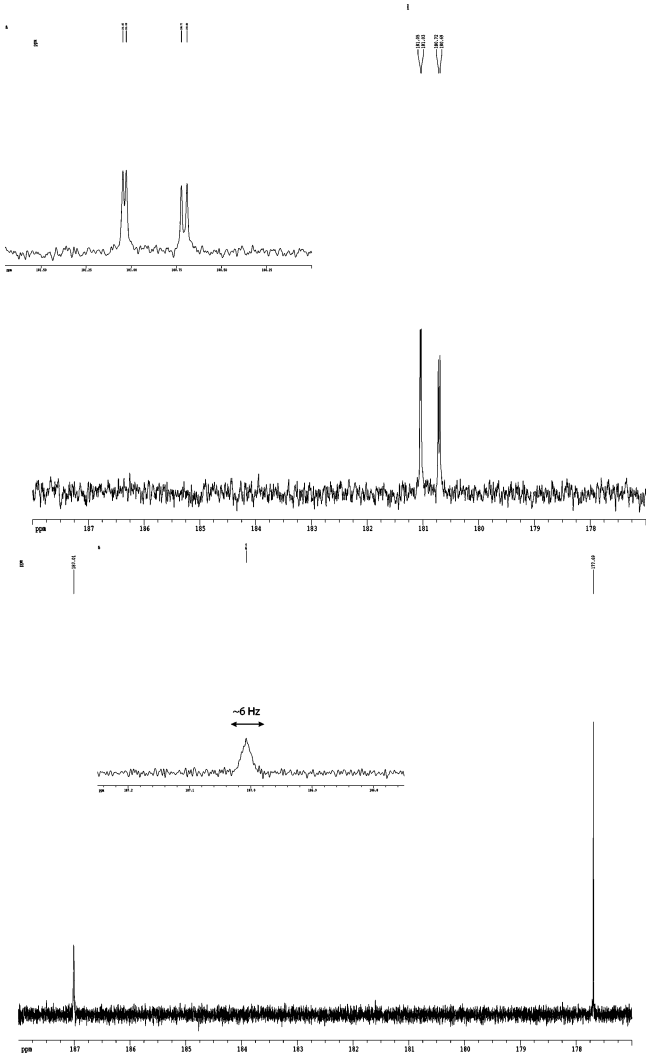

Figure 3. Carbonyl regions of the $^{13}C\{^1H\}$ NMR spectra of (a) **10*β*** and (b) **14** in THF-d_8.

broadened because of the fluxional nature of this intermediate, several important features were distinguishable. The ^1H NMR spectrum revealed that the methylene hydrogens assigned to the CH_2CH_2Pd fragment of BINAP complex **13** were also discernible in intermediate **27** at similar chemical shifts; the appropriate cross-peaks also were seen in the COSY spectrum. A broad peak at 9.03 ppm evidenced the isatin acetal N−H bond. Expanding the spectral width of the ^1H NMR spectrum of intermediate **27** to include the region from 25 to −15 ppm did not reveal any unusual peaks. The carbonyl peaks in the $^{13}C\{^1H\}$ NMR spectrum of intermediate **27** appear as narrow singlets at 179.04 and 175.51 ppm, paralleling their positions in Heck product **4** in THF-d_8 (177.49 and 174.39 ppm). As with palladacycles **3**, **10**, and **11**, the $^{31}P\{^1H\}$ NMR spectrum of intermediate **27** shows two doublets of approximately equal broadness; that is, the expected AB pattern associated with the two inequivalent phosphorus atoms of the coordinated (*R*)-BINAP [$^{31}P\{^1H\}$ NMR in THF-d_8: δ 43.4 (d, $^2J(P-P) = 50.5$ Hz), 17.7 (d, $^2J(P-P) = 49.5$ Hz)].

Discussion

Palladacycle Formation. The unique structural features of Heck cyclization precursors **2** and **9**, particularly the presence

Scheme 6

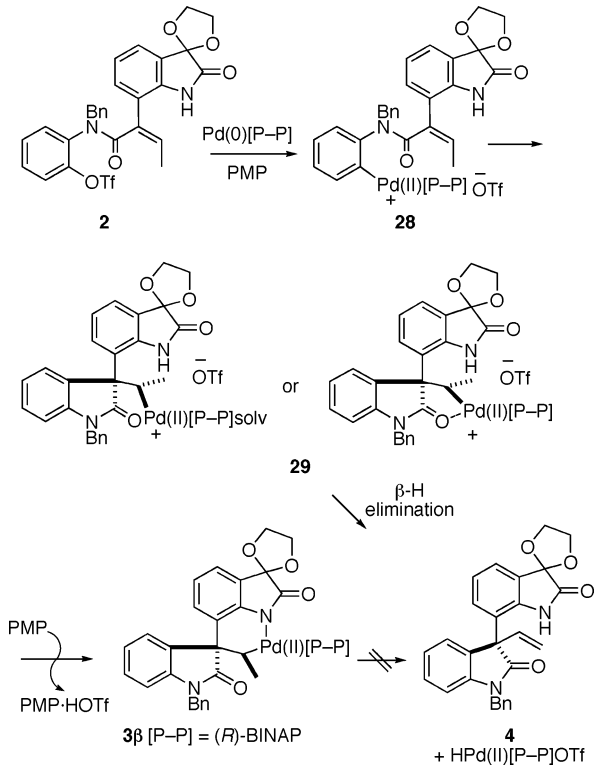

of multiple heteroatom functionality, are responsible for the formation of isolable palladacycles upon their reaction with Pd(0) bisphosphine complexes. The sequence by which palladacycles **3**, **10**, and **11** are believed to form is shown in Scheme 6 for the reaction of **2** with Pd[(*R*)-BINAP] (Pd(0)·[P−P]) in the presence of PMP.[50] Oxidative addition of Pd(0)[P−P] into the aryl triflate bond of **2** gives cationic Pd(II) intermediate **28**. Insertion of the palladium-aryl bond of **28** into the trisubstituted alkene in a 5-exo carbopalladation forms the quaternary center of cationic alkyl palladium intermediate **29**, which might be stabilized by coordination of the *N*-benzyloxindole carbonyl group.[51] In a typical Heck reaction, coordinatively unsaturated intermediate **29** undergoes β-hydride elimination, likely by way of an agostic species,[52] to generate terminal alkene **4** and a palladium(II) hydride complex. However, in the presence of the strong base PMP, the conjugate base of the oxindole coordinates to the Pd(II) center to generate the neutral six-membered palladacycle **3*β*** and PMP hydrotriflate at a rate faster than **29** suffers β-hydride elimination.[10,53] No ligand can readily dissociate from neutral palladacycle **3*β*** to generate a vacant coordination site for β-hydride elimination, thereby conferring unusual thermal stability (up to 140 °C) to this 16-electron complex. Although a wide variety of phosphine ligands were screened for palladacycle formation,[22] apparently only BINAP and BDPP have appropriate steric bulk and electron-donating

(50) (a) Amatore, C.; Jutand, A. *J. Organomet. Chem.* **1999**, *576*, 254−278. (b) Amatore, C.; Jutand, A. *Acc. Chem. Res.* **2000**, *33*, 314−321. (c) Casey, M.; Lawless, J.; Shirran, C. *Polyhedron* **2000**, *19*, 517−520. (d) von Schenck, H.; Åkermark, B.; Svensson, M. *J. Am. Chem. Soc.* **2003**, *125*, 3503−3508. (e) Hii, K. K.; Claridge, T. D. W.; Brown, J. M.; Smith, A.; Deeth, R. J. *Helv. Chim. Acta* **2001**, *84*, 3043−3056.

(51) Johnson, L. K.; Mecking, S.; Brookhart, M. *J. Am. Chem. Soc.* **1996**, *118*, 267−268.

(52) Schultz, L. H.; Brookhart, M. *Organometallics* **2001**, *20*, 3975−3982.

(53) It is also possible, though less likely, that the neutral oxindole fragment of **29** attacks the Pd(II) center directly to form an intermediate that then loses a proton to PMP.

Scheme 7

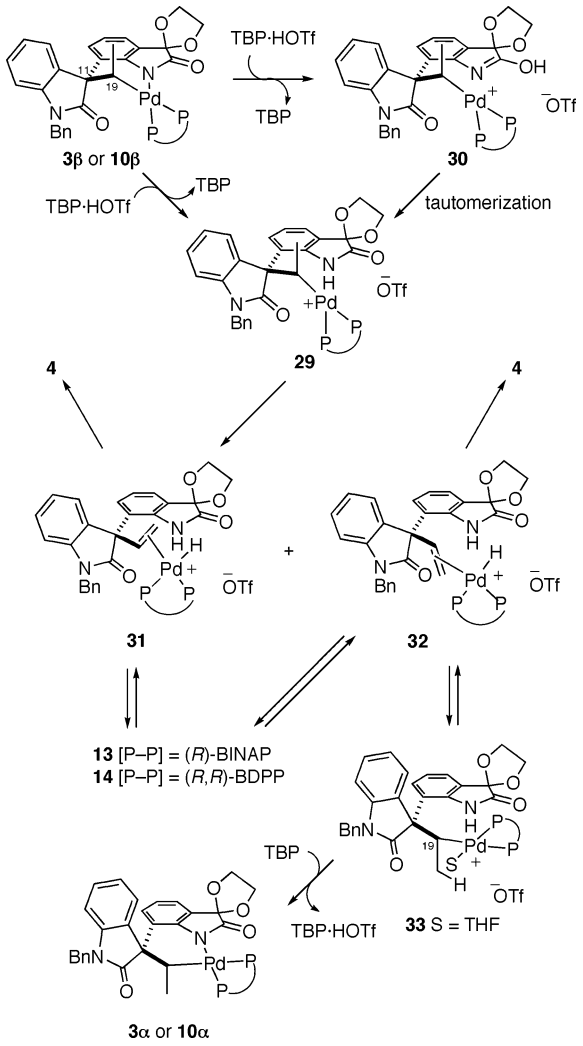

character to effectively stabilize the corresponding neutral palladacycles allowing for their isolation and handling.

Transformations of Palladacycles 3*β* and 10*β*. Epimerization of the palladium−carbon stereocenter of palladacycles **3*β*** and **10*β*** was observed under acidic and thermal reaction conditions. The observation of palladium complexes **13** and **14** during acid-promoted conversion of palladacycles **3*β*** and **10*β*** to their α-epimers suggests that they are likely intermediates in this process. Palladium complexes **13** and **14** were shown to have an isatin fragment containing a N−H bond, indicating that the acid-promoted epimerization proceeds by way of cationic Pd(II) intermediates (Scheme 7). Severing the Pd−N bond of **3*β*** (or **10*β***) by protonation of the isatin acetal with TBP·HOTf gives cationic Pd(II) intermediate **29**, which would be stabilized by coordination of the proximal *N*-benzyloxindole carbonyl oxygen or a THF solvent molecule or by an agostic-hydride interaction. In this conversion, protonation likely occurs at the carbonyl oxygen of **3*β*** (or **10*β***) to generate intermediate **30** after dissociation of the nitrogen ligand; tautomerization of **30** then would give cationic complex **29**.[54] *β*-Hydride elimination of this intermediate would yield Pd−alkene hydride complex **31**. Several reaction pathways would be open to this palladium hydride species. It could suffer decomplexation to generate Heck product **29** or progress on to generate the α-methyl palladacycle epimer **3α** (or **10α**). The most direct route for forming the α-methyl palladacycle epimer would involve equilibration of Pd−alkene hydride **31** with the diastereomeric Pd−alkene hydride complex **32**. Hydropalladation of the double bond of this latter intermediate from the *si* face would give secondary alkyl Pd(II) intermediate **33** having the inverted configuration at C19. Subsequent trapping of **33** by the oxindole nitrogen and loss of a proton to TBP would give palladacycle **3α** (or **10α**). It is reasonable to speculate that palladium complexes **13** and **14** provide an avenue for interconversion of Pd−alkene hydride complexes **31** and **32**.

Epimerization of the methyl substituent also was observed when palladacycles **3*β*** and **10*β*** were heated in DMF or DMA. Subjecting palladacycles **3α** and **10α** to thermal epimerization conditions did not lead to the corresponding *β*-methyl palladacycles. These observations, together with results of acid-promoted epimerizations, support the conclusion that epimerization of the methyl group from *β* to α is energetically downhill. Although no intermediates were detected in the thermal epimerizations of palladacycles **3*β*** and **10*β***, a heterolytic mechanism similar to that depicted in Scheme 7 cannot be rigorously ruled out. Nonetheless, such a heterolytic mechanism does not seem likely as neither DMF nor DMA are good proton donors. However, the acceleration of the epimerization in the presence of added H_2O suggests that a small amount of adventitious water in DMF or DMA could be acting as the proton donor, promoting a heterolytic reaction pathway. Epimerization by a homolytic cleavage of the palladium−carbon bond is also possible under the thermal conditions. The low yields of the epimerized palladacycles and the large amounts of decomposition products observed in these thermal reactions could be accounted for by the similar homolytic bond strengths of Pd−C, Pd−N, and Pd−P bonds.[55]

Assignment of Structures to Palladium Complexes 13, 14, and 27 and Postulated Mechanisms for Their Formation and Reaction. The ^{1}H NMR spectra of **13** and **14** reveal that a CH_2CH_2Pd fragment exists in these complexes. Incorporating an NMR-active ^{15}N label into the ketal-protected isatin fragment of **2** provided access to ^{15}N-labeled palladium complexes **[^{15}N]-13** and **[^{15}N]14**, ultimately serving to unambiguously rule out several possible structures for **13** and **14**. Whereas the nitrogen signals in the ^{15}N{^{1}H} NMR spectra of **[^{15}N]13** and **[^{15}N]14** appear as singlets, these signals are doublets in the corresponding ^{1}H-coupled ^{15}N NMR spectra with *J*-values consistent with one-bond N−H coupling. These data prove that **13** and **14** are cationic complexes in which the nitrogen atom of the isatin

(54) Unpublished results from this group are consistent with O-protonation. Thus, attempts to protect the isatin nitrogen of **4** resulted in exclusive reaction of electrophiles at oxygen:

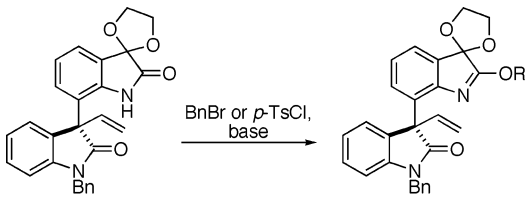

(55) Homolytic palladium bond strengths are often compared to the corresponding bond to hydrogen. See: Bryndza, H. E.; Fong, L. K.; Paciello, R. A.; Tam, W.; Bercaw, J. E. *J. Am. Chem. Soc.* **1987**, *109*, 1444−1456.

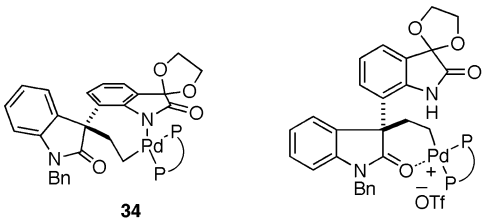

Figure 4. Proposed structures of cationic complexes **13** and **14** and a structure **34** that is ruled out.

acetal fragment is protonated, thus eliminating seven-membered palladacycles **34** as possible structures for these intermediates (Figure 4).[56]

Further insight into the structures of cationic complexes **13** and **14** was obtained from the $^{13}C\{^1H\}$ NMR and IR spectra of ^{17}O-labeled palladium complexes derived from precursor **[^{17}O]2**. Monitoring the reaction of **[^{17}O]3*β*** (or **[^{17}O]10*β***) with TBP·HOTf by $^{13}C\{^1H\}$ NMR revealed that carbonyl carbon C1 of the isatin acetal fragment is more shielded in **13** (and **14**) and the carbonyl carbon C12 of the *N*-benzyloxindole is slightly more deshielded compared to the position of these signals in starting palladacycles. Whereas the carbonyl carbons of the isatin acetal unit in **13** and **14** are singlets in the $^{13}C\{^1H\}$ NMR spectra, the carbonyl carbons of the oxindole are broad, complex multiplets. Additionally, the IR spectra of **13** and **14** exhibit unusually low frequency IR stretches for the oxindole carbonyls. The X-ray crystal structure of palladacycle **10*β*** shows that the *N*-benzyloxindole carbonyl oxygen is positioned to engage in a weak bonding interaction with the palladium atom. Taken as a whole, these observations lead to the assignment of **13** and **14** as the cationic palladacyclic complexes depicted in Figure 4. In these complexes, the alkylpalladium fragment would be stabilized toward *β*-elimination by coordination of the cationic palladium center with the neighboring *N*-benzyloxindole carbonyl group.

Further evidence in support of the structures assigned to cationic palladacycles **13** and **14** comes from our attempts to carbonylate neutral palladacycles **3*β*** and **10*β***. Direct carbonylation of **3*β*** and **10*β*** did not occur under neutral conditions; however, addition of 1 equiv of TBP·HOTf to MeOH solutions of either **3*β*** or **10*β*** under a CO atmosphere gave excellent yields of methyl ester **15** (eq 2). The rapid conversion of neutral palladacycle **3*β*** to cationic palladacycle **13** under these conditions is observed by $^{31}P\{^1H\}$ and ^1H NMR. Reversible dissociation of the weakly bound *N*-benzyloxindole ligand of cationic palladacycle **13** or **14** would generate an open coordination site for association of CO cis to the alkyl group. Insertion of CO into the palladium alkyl bond followed by methanolysis would provide the methyl ester **15** having the same carbon backbone as cationic palladacycles **13** and **14**. The cationic nature of palladacycles **13** and **14** is consistent with the consumption of 1 equiv of TBP·HOTf in their formation.

On the basis of the evidence outlined above, we propose the following mechanism for the formation of cationic Pd(II) complexes **13** and **14** (Scheme 8). Palladacycle ring-opening of 3*β* (or **10*β***) brought about protonation of the isatin fragment, which might be aided in an associative manner by the weak

Scheme 8

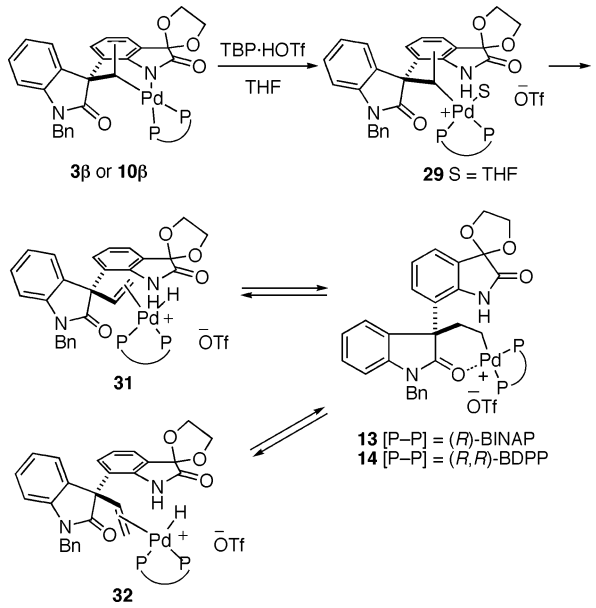

bonding interaction of the *N*-benzyloxindole oxygen, to generate cationic intermediate **29**. Rotation of the Pd−C *σ*-bond and *β*-H elimination occurs to give palladium hydride complex **31**. However, instead of dissociating, the double bond of this intermediate suffers regioisomeric hydropalladation.[57] Coordination of the opportunely positioned *N*-benzyloxindole carbonyl oxygen then gives the amide-bound six-membered palladacycles **13** and **14** as shown.[11b,58,59] This structural formulation for cationic complexes **13** and **14** is consistent with their postulated role in the interconversion of Pd−alkene hydride complexes **31** and **32** as *β*-hydride elimination of these complexes could generate either diastereomeric Pd−alkene hydride complex.

Allowing a solution of cationic palladacycle **13** and THF-d_8 to react with 1 equiv of TBP·HOTf resulted in the rapid formation of a transient intermediate **27** that contains a Pd·BINAP fragment (Scheme 9). The $^{13}C\{^1H\}$ NMR spectrum of **27** reveals that the chemical shifts of the carbonyl carbons are similar to those in *β*-hydride elimination product **4**. Both

(56) Such neutral palladacycles would arise from intermediate **32** by reinsertion of Pd−H to the vinyl group in the alternate sense.

(57) Albéniz, A. C.; Espinet, P.; Lin, Y.-S. *Organometallics* **1996**, *15*, 5010−5017.

(58) (a) Lee, S.; Hartwig, J. F. *J. Org. Chem.* **2001**, *66*, 3402−3415.

(59) In cationic palladacycles **13** and **14**, the *N*-benzyloxindole fragment can potentially bind to the palladium center via the oxygen or via the nitrogen. Although the [3.2.1] bridged palladacyclic structure **B** in which nitrogen is bound to palladium looks highly strained, the hand-held model is not considerably more strained than fused bicyclic structure **A**. On the basis of soft−soft interactions, coordination of palladium to the softer nitrogen atom would be expected. Although no X-ray structural information could be obtained for cationic palladacycles **13** and **14**, spectroscopic data, in particular the $^{13}C\{^1H\}$ and ^1H NMR spectra, provide strong evidence that suggests this is not the favored coordination mode. The benzyl carbon attached to the nitrogen of the *N*-benzyloxindole appears as a slightly broadened singlet in each carbon spectrum, and the benzyl hydrogens appear as a simple AB system. If the nitrogen was directly coordinated to palladium (structure **B**), it is anticipated that the benzyl carbon and benzyl protons would couple to the two phosphorus atoms in the bidentate ligands on palladium, giving doublets of doublets instead of the observed singlets. Additionally, in structure **A** the amide is fully conjugated, whereas in structure **B** it is not.

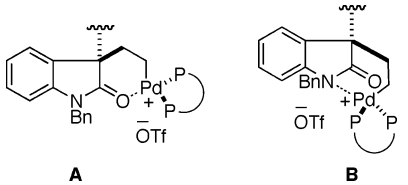

Scheme 9

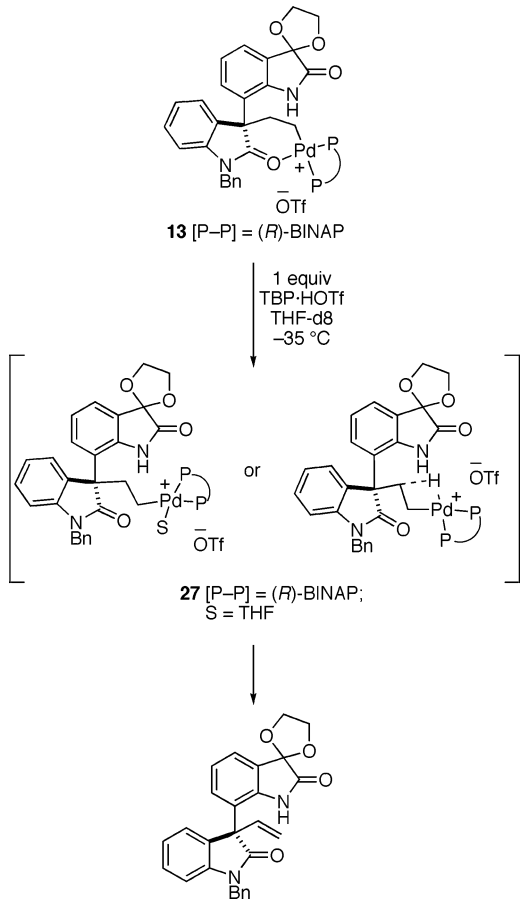

carbonyl peaks appear as sharp singlets, indicating that neither is coupling to phosphorus. The $^{13}C\{H\}$ and ^{1}H NMR spectra show that the CH_2CH_2 fragment is still intact as signals for this fragment appear at shifts similar to those seen in cationic palladacycles **13** and **14** and not at positions expected for a Pd(II)−alkene complex.[60] One of the four methylene hydrogens is not discernible in the ^{1}H NMR spectrum, but cross-peaks to the other three methylene hydrogens in the COSY spectrum indicate that it lies under the THF solvent peak at ∼1.8 ppm. The chemical shifts of the phosphorus atoms in the $^{31}P\{^{1}H\}$ NMR spectrum are typical of a palladium complex in which one phosphorus atom is trans to a carbon atom and the other trans to a more electronegative substituent. Because THF is a coordinating solvent, it likely occupies the fourth coordination site of cationic complex **27**. A *β*-agostic structure for **27** is possible; however, no evidence was found for a hydrogen between 0 to −15 ppm.[61] The propensity of palladium complex **27** to undergo rapid *β*-hydride elimination at ambient temperature is consistent with the formulation of the CH_2CH_2Pd fragment of **27** as an acyclic unit, as diminished thermal stability would be expected if a palladacyclic ring were not present. Why the addition of 1 equiv of TBP·HOTf promotes the conversion of palladacycle **13** to intermediate **27** is less clear.[62]

(60) (a) Shultz, C. S.; Ledford, J.; DeSimone, J. M.; Brookhart, M. *J. Am. Chem. Soc.* **2000**, *122*, 6351−6356. (b) Malinoski, J. M.; White, P. S.; Brookhart, M. *Organometallics* **2003**, *22*, 621−623.

(61) For spectroscopic characterization of several cationic diimine Pd(II) *β*-agostic complexes in the context of polymerization reactions, see: Shultz, L. H.; Tempel, D. J.; Brookhart, M. *J. Am. Chem. Soc.* **2001**, *123*, 11539−11555.

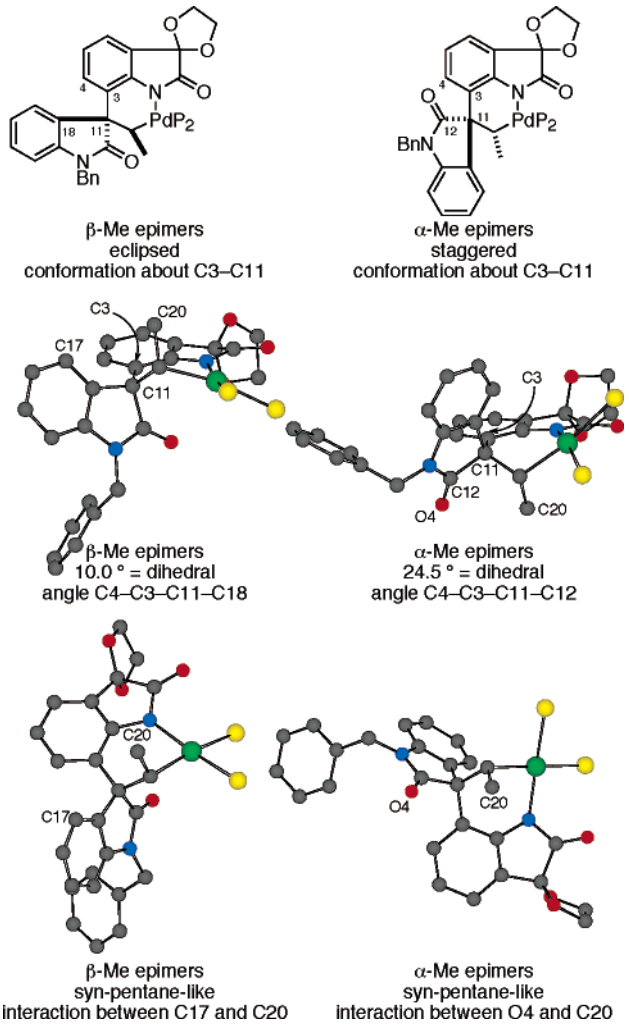

Figure 5. Steric argument for the thermodynamically favored α-methyl palladacycles. The hydrogen atoms and the substituents on the phosphorus atoms have been removed for clarity.

Rationale for the Thermodynamic Stability of the α-Methyl Epimers. The α-methyl epimers of palladacycles **3** and **10** are more stable than their *β*-methyl counterparts. Examination of the solid-state structures of a member of each epimer family provides insight into the energy differences between the methyl epimers. The solid-state structures for **3α** and **10*β*** are shown in Figure 5, with the substituents on the phosphorus atoms removed for clarity. The palladacyclic rings adopt different sofa conformations in the two structures, each placing the methyl group pseudoaxial. The axial disposition of the methyl substituent avoids severe steric interactions between this group and the phenyl substituents of the bisphosphine ligands. Thus, the C12 carbonyl carbon is axial in the *β*-epimer and equatorial in the α-epimer, vice-versa for the aryl carbon C17 of the spirooxindole fragment. In the *β*-epimer, the substituents about the C11−C3 bond are almost eclipsed, as evidenced by the small dihedral angle between C4−C3−C11−C18 (10.0°). This conformation of the *β*-epimer has a syn-pentane-like interaction between C17 and C20. In the α-methyl epimers, substituents about C11−C3 are more staggered with the dihedral angle between C4−C3−C11−C12 being 24.5°. Although a syn-pentane-like interaction exists between the O4 and C20 in the

(62) Perhaps hydrogen bonding of the ammonium salt to the oxindole carbonyl group disrupts coordination of the *N*-benzyloxindole ligand.

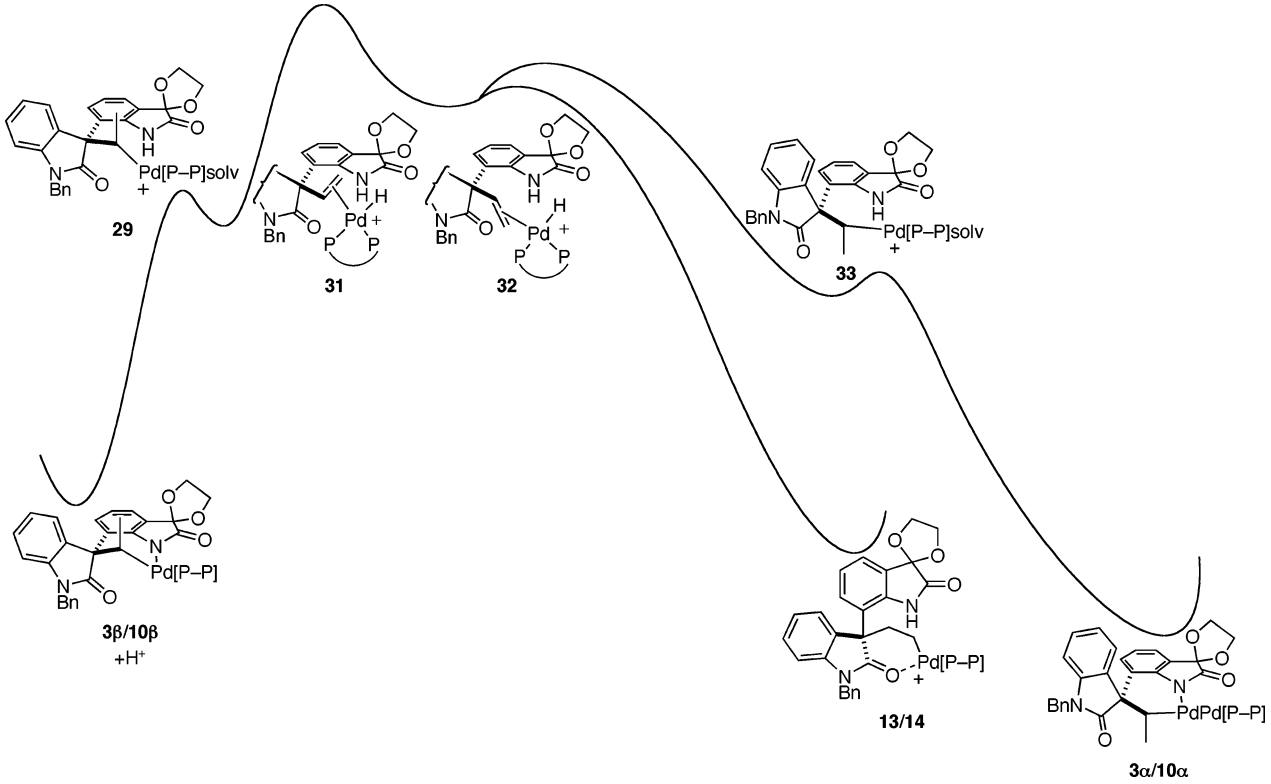

Figure 6. Relative energy diagram.

α-methyl epimer, this interaction should be much less destabilizing than the interaction between C17 and C20 in the *β*-methyl epimer.

A diagram relating the relative energy of the palladium complexes characterized or implicated in this study is shown in Figure 6. The greater stability of cationic complexes **13** and **14** relative to **29** undoubtedly derives from the greater stability of a primary- than a secondary-carbon *σ*-bond.[63] Perhaps this difference is further enhanced by greater stability of a six-membered, rather than a five-membered, palladacyclic ring that incorporates an oxindole fragment.[64] That the conversion of **29** to **13**/**14** would be downhill in energy and rapid is supported by the studies of Brown and co-workers.[65] The initial observation of cationic palladacycles **13** and **14** in the acid-promoted epimerization reactions of palladacycles **3*β*** and **10*β*** indicates that the energy barrier for hydropalladation of palladium hydride alkene complexes **31** and **32** to give a primary alkyl palladium species is lower than that for hydropalladation of **32** to give a secondary alkyl palladium species en route to **3α**/**10α** as **33** is not observed.[66] The eventual formation of the α-methyl palladacycles **3α** and **10α** in the acid-promoted epimerization reactions of palladacycles **3*β*** and **10*β*** shows that the cationic primary palladium alkyl **13**/**14**, the cationic alkene−palladium hydride complexes **31** and **32**, and the cationic secondary palladium alkyl **33** are in rapid equilibrium. The neutral seven-membered palladacycle **34**, which could have been generated by deprotonation of **13**/**14**, is apparently much less stable than the six-membered ring α-methyl palladacycles **3α**/**10α**; thus, it is not observed.

Conclusions

A series of enantiomerically enriched palladacycles containing palladium bonded to a stereogenic carbon and an N-coordinated oxindole was synthesized in high yield and diastereoselectivity. X-ray crystallographic studies of two of these chiral palladacyclic complexes reveal a proclivity of the major palladacyclic diastereomer to form a weak axial bonding interaction with the carbonyl oxygen of a neighboring *N*-benzyloxindole substituent. These unusual palladium alkyls, which have three accessible *β*-hydrogens, are thermally stable at temperatures as high as 120 °C. At higher temperature, or at room temperature in the presence of weak acids, these complexes epimerize at the stereogenic carbon bonded to palladium. Stabilizing coordination of the *N*-benzyloxindole carbonyl group is seen in the rapid conversion of neutral six-membered palladacycles **3*β*** and **10*β*** to cationic six-membered palladacycles **13** and **14** in the presence of a weak acid and is likely also involved in stabilizing intermediates en route to Heck product **4**, in particular alkene−palladium hydride intermediates **31** and **32**. A novel mechanism for epimerization of a palladium-bound stereogenic carbon is revealed in these studies, in which cationic palladium alkyls **13**/**14** and **33** and cationic palladium hydride alkene complexes **31** and **32** are in rapid equilibrium.

Experimental Section

(*R*,*R*)-BDPP Palladacycle (10*β*). A base-washed, oven-dried sealed tube equipped with a magnetic stirring bar and a Teflon seal was charged with aryl triflate **2** (75.0 mg, 127 *μ*mol), $Pd(OAc)_2$ (29.0 mg, 127 *μ*mol), and (2*R*,4*R*)-(+)-2,4-bis(diphenylphosphino)pentane [(*R*,*R*)-BDPP, 112 mg, 254 *μ*mol]. Deoxygenated *N*,*N*-dimethylacetamide

(63) Cf., Jones, W. D.; Feher, F. J. *Acc. Chem. Res.* **1989**, *22*, 91−100.
(64) A related thermodynamic preference of a six-membered chelate was observed in cationic Pd(diimine) complexes chelated by an ester carbonyl fragment; see ref 51.
(65) (a) Brown, J. M.; Pérez-Torrente, J. J.; Alcock, N. W.; Clase, H. J. *Organometallics* **1995**, *14*, 207−213. (b) Brown, J. M.; Hii, K. K. *Angew. Chem.* **1996**, *35*, 657−659. (c) Hii, K. K.; Claridge, T. D. W.; Brown, J. M. *Angew. Chem.* **1997**, *36*, 984−987. (d) Reference 50e.
(66) This low barrier to migration is substantiated by DFT calculations in related cationic Pd(II) systems; see ref 50e.

(DMA, 1.3 mL, distilled from CaH_2 into a sealed tube under reduced pressure, backfilled with Ar, then sparged with Ar for 2 h) and 1,2,2,6,6-pentamethylpiperidine (PMP, 79 mg, 510 μmol, distilled from CaH_2 under Ar into a sealed tube under reduced pressure and backfilled with Ar) were added to the solids. A stream of Ar was bubbled through the resulting mixture for 15 min, and then the sealed tube was flushed with a steady stream of Ar for an additional 15 min. The tube was sealed and maintained at 70 °C for 16 h. The solution was allowed to cool to room temperature, diluted with EtOAc (25 mL), and poured into saturated aqueous $NaHCO_3$ (25 mL). The aqueous phase was separated and extracted with EtOAc (75 mL). The combined organic extracts were dried (Na_2SO_4) and concentrated onto silica gel. This residue was immediately purified by flash chromatography eluting with 50−100% diethyl ether−hexanes to afford **10*β*** (118 mg, 119 μmol, 94%) as a colorless solid: mp 170 °C with decomposition (from Et_2O−hexanes); ^{1}H NMR (500 MHz, $CDCl_3$): δ 8.18 (br m, 2H, Ar*H*), 7.77 (t, J = 8.8 Hz, 2H, Ar*H*), 7.59 (t, J = 8.9 Hz, 2H, Ar*H*), 7.39 (d, J = 7.4 Hz, 2H, Ar*H*), 7.31−7.12 (m, 12H, Ar*H*), 7.02−6.89 (m, 6H, Ar*H*), 6.77−6.74 (m, 3H, Ar*H*), 6.67 (d, J = 7.8 Hz, 1H, Ar*H*), 6.49 (t, J = 7.6 Hz, 1H, Ar*H*), 6.27 (d, J = 7.9 Hz, 1H, Ar*H*), 5.27 (d, J = 15.3 Hz, 1H, CH_2), 4.62 (d, J = 15.3 Hz, 1H, CH_2), 4.20−4.16 (m, 1H, CH_2), 3.90 (dd, J = 13.8, 6.9 Hz, 1H, CH_2), 3.71−3.67 (m, 1H, CH_2), 3.51 (dd, J = 13.8, 7.3, 1H, CH_2), 2.82−2.72 (m, 1H, C*H*), 2.71−2.61 (m, 1H, C*H*), 2.00−1.81 (m, 2H, CH_2), 1.59−1.51 (m, 4H, CH_3, C*H*), 1.07 (ddd, J = 10.5, 6.9, 3.8 Hz, 3H, CH_3), 0.94 (dd, J = 10.7, 7.2 Hz, 3H, CH_3); ^{13}C NMR (125 MHz, $CDCl_3$): δ 180.54 (dd, ^3J(C,P) = 2.4, 0.5 Hz), 180.32 (d, ^4J(C,P) = 1.8 Hz), 152.84, 142.36, 136.69, 136.62 (2C), 136.52, 135.05, 134.94, 134.30, 134.05, 132.08, 131.99, 131.70, 131.64, 131.23, 130.87, 130.45, 130.22 (m, 3C), 128.89−127.76 (m, 14C), 126.72, 124.82, 124.03, 122.24, 121.66, 119.15, 108.26, 104.25, 104.21, 65.19, 64.38, 59.73, 44.23, 42.30 (dd, ^2J(C,P) = 95.3, 6.3 Hz), 35.97 (br), 29.29 (dd, J(C,P) = 19.9, 1.4 Hz), 25.84 (dd, J(C,P) = 23.1, 3.2 Hz), 20.15 (dd, ^3J(C,P) = 7.9, 1.0 Hz), 18.62 (dd, J(C,P) = 4.2, 2.3 Hz), 15.66 (d, J(C,P) = 8.8 Hz); ^{31}P NMR (162 MHz, $CDCl_3$): δ 28.50 (d, ^2J(P,P) = 58.4 Hz, 1.00P), 9.31 (d, ^2J(P,P) = 58.5 Hz, 0.91P); $[\alpha]_{589}$ = −268, $[\alpha]_{577}$ = −284, $[\alpha]_{546}$ = −330, $[\alpha]_{435}$ = −684, $[\alpha]_{405}$ = −918 (*c* 1.0, $CHCl_3$); IR (thin film): 3057, 2964, 2930, 2899, 2853, 1698, 1671, 1598, 1486, 1467, 1432, 1343, 1297, 1235, 1181, 1127, 1100, 1000, 942, 745, 699 cm^{-1}; LRMS (ESI+) Calcd for $C_{56}H_{53}N_2O_4P_2Pd$ $(M + H)^+$: 985.25. Found: 985.28. X-ray quality crystals were obtained from a solution of **10*β*** in Et_2O (See Supporting Information).

Cationic (*R*,*R*)-BDPP Palladacycle (14). A solution of 2,6-di-*tert*-butylpyridine hydrotriflate (26 mg, 76 μmol) in deoxygenated THF-d_8 (0.2 mL) was added to a solution of **10*β*** (25 mg, 25 μmol) in deoxygenated THF-d_8 (0.6 mL) in an NMR tube under a steady stream of Ar. After <45 s, quantitative conversion to **14** was confirmed by ^{31}P and ^{1}H NMR analysis: ^{1}H NMR (500 MHz, THF-d_8): δ 9.27 (br s, 1H, N*H*), 7.97−6.85 (m, 31H, Ar*H*), 6.34 (d, J = 7.6 Hz, 1H, Ar*H*), 4.88 (d, J = 15.6 Hz, 1H, CH_2), 4.83 (d, J = 15.6 Hz, 1H, CH_2), 4.51−4.41 (m, 2H, CH_2), 4.40−4.16 (m, 2H, CH_2), 3.14−2.61 (m, 2H, C*H*), 1.98−1.84 (m, 3H, CH_2), 1.79−1.72 (m, 1H, CH_2), 1.23−1.14 (m, 3H, CH_3), 1.10−1.02 (m, 3H, CH_3), two methylene protons of the ligand are obscured; ^{13}C NMR (125 MHz, THF-d_8): δ 185.12 (br m), 175.82, 167.73 (br), 148.86 (br), 142.20, 141.39, 136.69 (d, J(C,P) = 12.0 Hz), 136.11, 135.80 (d, J(C,P) = 10.6 Hz), 135.62, 135.15, (d, J(C,P) = 9.7 Hz), 133.79 (d, J(C,P) = 10.6 Hz), 132.31, 132.04 (d, J(C,P) = 2.3 Hz), 131.96, 131.72, 131.37 (d, J(C,P) = 2.3 Hz), 130.25, 130.12, 130.03, 129.90, 130.08 (d, J(C,P) = 11.1 Hz), 128.70, 130.35−129.26 (m, 8C), 128.95, 128.29 (br), 127.46 (m, 2C), 126.10 (d, J(C,P) = 13.4 Hz), 124.35 (d, J(C,P) = 8.8 Hz), 123.86−122.70 (m, 4C), 122.23, 121.11, 112.65, 101.61, 66.79, 66.69, 61.53 (d, ^4J(C,P) = 2.3 Hz), 45.76 (br), 36.36 (dd, ^2J(C,P) = 9.7, 1.8 Hz), 33.85 (br m), 30.78, 28.19 (dd, J(C,P) = 31.9, 8.8 Hz), 18.09 (br), 17.67 (d, J(C,P) = 2.3 Hz), 15.85; ^{31}P NMR (202 MHz, THF-d_8): δ 46.3 (d, ^2J(P,P) = 59.2 Hz, 1.00P), 10.6 (d, ^2J(P,P) = 59.4 Hz, 1.04P); IR (thin film): 2972, 2907, 2980, 1741/1735, 1640, 1617, 1577, 1532, 1486, 1468, 1440, 1413, 1374, 1251, 1224, 1154, 1100, 1031, 946, 888, 818, 749, 699 cm^{-1}; LRMS (ESI+) Calcd for $C_{56}H_{53}N_2O_4P_2Pd$ (M^+): 985.25. Found: 985.18.

Acknowledgment. We wish to thank Professor Alan Heyduk for helpful discussions, Professor Melanie Cocco and Dr. Bao Dao Nguyen for their assistance with ^{13}C{^{1}H} NMR experiments with ^{31}P-isotope selection, Dr. Scott Ross and Ms. Catherine Larsen of California Institute of Technology for assistance with early broadband ^{31}P-decoupled ^{13}C{^{1}H} NMR experiments, and Dr. Joe Ziller for solving the structures of palladacycles **3α** and **10*β***. This research was supported by the National Science Foundation (CHE-9726471). NMR and mass spectra were determined at UCI with instruments purchased with the assistance of NSF and NIH shared instrumentation grants.

Supporting Information Available: Experimental procedures and characterization data for the preparation of **3*β***, **3α**, ***ent*-3*β***, **6**, **7**, **9**, **10*β***, ***ent*-10*β***, **11*β***, **12**, **13**, **14**, **15**, and spectral evidence for **27**. High-resolution mass spectrometric data for ^{15}N-labeled compounds **17**, **21**, **[^{15}N]8**, and **[^{15}N]2** and ^{17}O-labeled compounds **24**, **[^{17}O]5**, **25**, **[^{17}O]22**, and **[^{17}O]2**. Infrared spectra for **3*β***, **13**, **10*β***, **14**, **[^{17}O]3*β***, **[^{17}O]13**, **[^{17}O]10*β***, **[^{17}O]14** (PDF). X-ray crystallographic data for compounds **3α** and **10*β*** (CIF). This material is available free of charge via the Internet at http://pubs.acs.org.

JA045047P